



Evidence for a “Little Ice Age” glacial advance within the Antarctic Peninsula – Examples from glacially-overrun raised beaches

Alexander R. Simms^{a,*}, Michael J. Bentley^b, Lauren M. Simkins^c, Julie Zurbuchen^a,
Laura C. Reynolds^e, Regina DeWitt^d, Elizabeth R. Thomas^f

^a Department of Earth Science, University of California Santa Barbara, 1006 Webb Hall, Santa Barbara, CA 93106, USA

^b Department of Geography, Durham University, Durham DH1 3LE, UK

^c Department of Environmental Sciences, University of Virginia, Clark Hall 205, 291 McCormick Road, Charlottesville, VA 22904, USA

^d Department of Physics, East Carolina University, Howell Science Complex, Rm C-209, 1000 E. 5th Street, Greenville, NC 27858, USA

^e Department of Earth, Environment, and Physics, Worcester State University, 486 Chandler St., Worcester, MA 01602, USA

^f Ice Dynamics and Paleoclimate, British Antarctic Survey, Cambridge CB3 0ET, UK

ARTICLE INFO

Article history:

Received 30 June 2021

Received in revised form

11 September 2021

Accepted 14 September 2021

Available online xxx

Handling Editor: C. O’Cofaigh

Keywords:

Neoglacial
Antarctica
Climate change
Holocene
Coast
Sea level
Shallow marine
Glacial advance

ABSTRACT

Recognition of how dynamic the Antarctic ice sheets and glaciers were during the late Holocene has grown in recent years. Proxy data suggests the presence of Neoglacial advances but few moraines or glacial features from this time have been dated compared to glaciated landscapes of the Northern Hemisphere. Debate continues on whether parts of Antarctica experienced glacial advance at the same time as the “Little Ice Age” (LIA), which is well-documented in the Northern Hemisphere. We provide new evidence for late Holocene glacial fluctuations at three locations along the Antarctic Peninsula. A moraine or till sheet from a tidewater glacier cross cuts a series of dated raised beaches at Tay Head, Joinville Island along the northwestern Weddell Sea. At Spark Point, on Greenwich Island, a glacier has overrun Holocene raised beaches and a shell-bearing marine deposit is reworked into a glacial diamicton. A third site in Calmette Bay within the larger Marguerite Bay also contains a recent moraine that cuts across a series of dated raised beach ridges. The new ages constraining these glacial advances are in broad agreement with the handful of other existing ages on moraines and proxy records suggestive of cooler conditions within the Antarctic Peninsula. Combining available timing constraints into a Bayesian model yields an age of 400 to 90 cal BP (1550–1860 CE; 95%) for the LIA across the Antarctica Peninsula. Consideration of a two-phase glacial advance within our Bayesian framework does fit more of the data from across the Antarctic Peninsula and suggests advances from 575 to 330 cal BP (1375–1620 CE) and 400 to 50 cal BP (1550–1900 CE). However, more work is needed to determine if such a two-phase advance occurred. Regardless, its similar timing within the Antarctic Peninsula to that of the Northern Hemisphere supports recent assertions of a volcanic or solar forcing for the LIA. These recent readvances also provide a possible mechanism for changes in the rates of Holocene relative sea-level change recorded across the Antarctic Peninsula suggesting that the Antarctic ice sheets may have been more responsive to past climate changes than previously thought and glacial isostatic adjustment from the LIA and possibly other Holocene glacial oscillations is superimposed upon the longer relaxation from the Last Glacial Maximum.

© 2021 The Authors. Published by Elsevier Ltd. This is an open access article under the CC BY license (<http://creativecommons.org/licenses/by/4.0/>).

1. Introduction

The Antarctic ice sheets are the largest reservoirs of freshwater and potential sea-level rise on the planet, and play an important

role in governing Earth’s climate and ocean circulation. However, despite a growing body of literature supporting the occurrence of glacial oscillations through the Holocene (Wanner et al., 2011), many questions remain as to the geographic range and timing of these oscillations. One important question that remains is whether a “Little Ice Age” (LIA) event occurred within Antarctica (Bentley et al., 2009). Best defined around the North Atlantic, the LIA was a period of relatively cool temperatures characterized by localized

* Corresponding author.

E-mail address: asimms@geol.ucsb.edu (A.R. Simms).

glacial advances throughout Northern Europe and North America (Grove, 2004; Mann et al., 2009) from approximately 1500 to 1800 CE (PAGES 2k Consortium, 2013). Numerical models simulating land-based glacial responses to ice-core derived temperature trends suggest that atmospheric cooling likely led to glacial advances in Antarctica during the Northern Hemisphere LIA (Davies et al., 2014). A handful of studies have found evidence for Antarctic glacial advances within the last ~500 years (e.g. Clapperton and Sugden, 1988; Hall, 2007; Guglielmin et al., 2016; Kaplan et al., 2020), but they could have occurred asynchronously due to local effects (PAGES 2k Consortium, 2013). Alternatively, they could be archives of a true, yet undetermined, synchronous LIA glacial advance in the Antarctic Peninsula.

Determining the timing and existence of a LIA in Antarctica is important for understanding drivers and rates of past climate change, and, by association, testing models of future glacial behavior (Davies et al., 2014). Discussion on the cause of the LIA is ongoing with suggested drivers including a decrease in CO₂ (refuted in Etheridge et al., 1996), changes in ocean circulation (Broecker, 2000), a decrease in solar activity (Nesme-Ribes and Mangeney, 1992), or an increase in volcanic activity (Miller et al., 2012; Bronnimann et al., 2019), with the latter having gained the most support in recent years (Owens et al., 2017; Mann et al., 2021). The cause of the LIA may also be a complex interplay of and feedbacks among several of these mechanisms (Kreutz et al., 1997; Zhong et al., 2011) including the role of large-scale modes of variability, such as the Interdecadal Pacific Oscillation (IPO), which has recently been linked to the LIA in the Antarctic Peninsula (Porter et al., 2021). The timing and geographic range of the LIA may provide clues as to its driver (Owens et al., 2017) and the sensitivity of glaciers to those forcings. For example, a near synchronous and globally widespread LIA has often been used to support assertions of a solar or volcanic driver (Miller et al., 2012), while its absence in Antarctica has been used as evidence for a “see-saw” like effect pointing to changes in ocean circulation as the driver (Broecker, 2000). Therefore, it is essential to develop paleo-climate records across a wide range of latitudes and regions (Jones et al., 2001). The Southern Hemisphere (Bradley and Jones, 1993) and the Antarctic in particular (Bentley et al., 2009) are short on records of glacier behavior across the period encompassed by the LIA. The purpose of this study is to provide new age constraints on a recent advance at three locations across the Antarctic Peninsula and compare these ages with those of other regional records of recent advances and cooler temperatures to provide additional data on climate oscillations across Antarctica over the last millennia.

2. Background

2.1. Geographic and climatic setting

The Antarctic Peninsula is one of the fastest warming locations in the world, with surface temperatures increasing by over 2.5 °C during the latter half of the 20th century (Vaughan et al., 2003). It experiences a maritime subpolar climate and contains several ice-free islands and peninsulas most notably the South Shetland Islands, the islands around James Ross Island in the Eastern Antarctic Peninsula (EAP), and the islands in and around Marguerite Bay. Today the region experiences significant differences in climate on its western and eastern sides (Reynolds, 1981; Morris and Vaughan, 2003; van Wessem et al., 2016). The western Antarctic Peninsula (WAP) is more heavily influenced by warmer south Pacific waters and storms while the EAP is more influenced by the isolated and colder Weddell Sea (Reynolds, 1981; Barbara et al., 2016). As a result, isotherms dip farther south on the WAP than the EAP making the WAP warmer and causing it to experience

higher rates of precipitation (Reynolds, 1981; Morris and Vaughan, 2003; Thomas et al., 2015, 2017, 2017; van Wessem et al., 2016).

The Antarctic Peninsula proper is a narrow spine of mountains approximately 300 km wide at its junction with the rest of West Antarctica south of Alexander Island that narrows to less than 50 km at its tip near the South Shetland Islands (Fig. 1). The central mountain range is largely the product of collisional tectonics, most recently as the Phoenix plate and Aluk Ridge subducted beneath the Peninsula's western margin through much of the Cenozoic (Anderson, 1999; Jordan et al., 2020). Subduction initially stopped in the south and the cessation migrated northward, such that active subduction is now only ongoing beneath the South Shetland Islands (Larter and Barker, 1991; Anderson, 1999). Glacial erosion of the inner shelf has left the peninsula lined with a series of archipelagos separated by deep troughs, on both its eastern and western sides (Anderson, 1999). An ice sheet feeding several outlet and tidewater glaciers runs the length of the Peninsula with localized ice caps covering most of the islands surrounding the peninsula. Major ice shelves today include the Larsen Ice Shelf along the EAP, ice shelves along the west side of Alexander Island, and the George VI Ice Shelf between the WAP and Alexander Island. These and many former ice shelves have retreated or disappeared over the last 50 years (Scambos et al., 2003).

2.2. General ice history

The Antarctic Peninsula has experienced several phases of glacial advances and retreat since the ice sheet began to retreat from its Last Glacial Maximum configuration at approximately 18.0 ka (Heroy and Anderson, 2007; O'Coifagh et al., 2014; Palacios et al., 2020; Kaplan et al., 2020). By ~10–8 ka, ice free areas emerged that have largely remained until present (Bentley et al., 2005, 2011, 2014, 2011; Johnson et al., 2011; Sterken et al., 2012; Hodgson et al., 2013; Oliva et al., 2016). Minor periods of readvance appeared to have occurred around 7 ka, 5 ka, and within the last 2.5 ka (Hall, 2009; Simms et al., 2011b, 2012; Davies et al., 2017; Palacios et al., 2020; Kaplan et al., 2020). The latter of these events, commencing at ~2.5 ka, is the so-called Neoglacial and is marked by cooler conditions (Sterken et al., 2012; Hodgson et al., 2013; Cejka et al., 2020), expansion of ice shelves (Pudsey et al., 2006; Christ et al., 2015), and glacial advances (Wolff et al., 2016; Palacios et al., 2020).

2.3. LIA and Antarctica

The LIA is a period ostensibly between about 1500 and 1800 CE in which global climate was cooler than today (Grove, 2004; Matthews and Briffa, 2005; PAGES 2k Consortium, 2013). In many locations it started abruptly (Miller et al., 2012) but was not marked by cold conditions throughout its entire 300–400 year duration (Kreutz et al., 1997; Mann and Jones, 2003) and consisted of multiple separate advances (Luckman, 2000). It is best recorded in historical records of glacial advance in the European Alps (Grove, 2004), but has been recorded across most continents (PAGES 2k Consortium, 2013). It represented a global cooling of approximately 0.5 °C (Mann et al., 2009; PAGES 2k Consortium, 2013), a much smaller magnitude cooling compared to that of the Last Glacial Maximum (5.5 °C). For this reason among others, some authors have called for a discontinuance of the use of the term (Ogilvie and Jonsson, 2001; Matthews and Briffa, 2005).

Several ice core records suggest cooling over this time period (Mosley-Thompson and Thompson, 1990; Thompson et al., 1994; Kreutz et al., 1997; Zhang et al., 2002; Li et al., 2009; Bertler et al., 2011; Orsi et al., 2012), while others do not (Thompson et al., 1994). Composite temperature reconstructions based on ice core

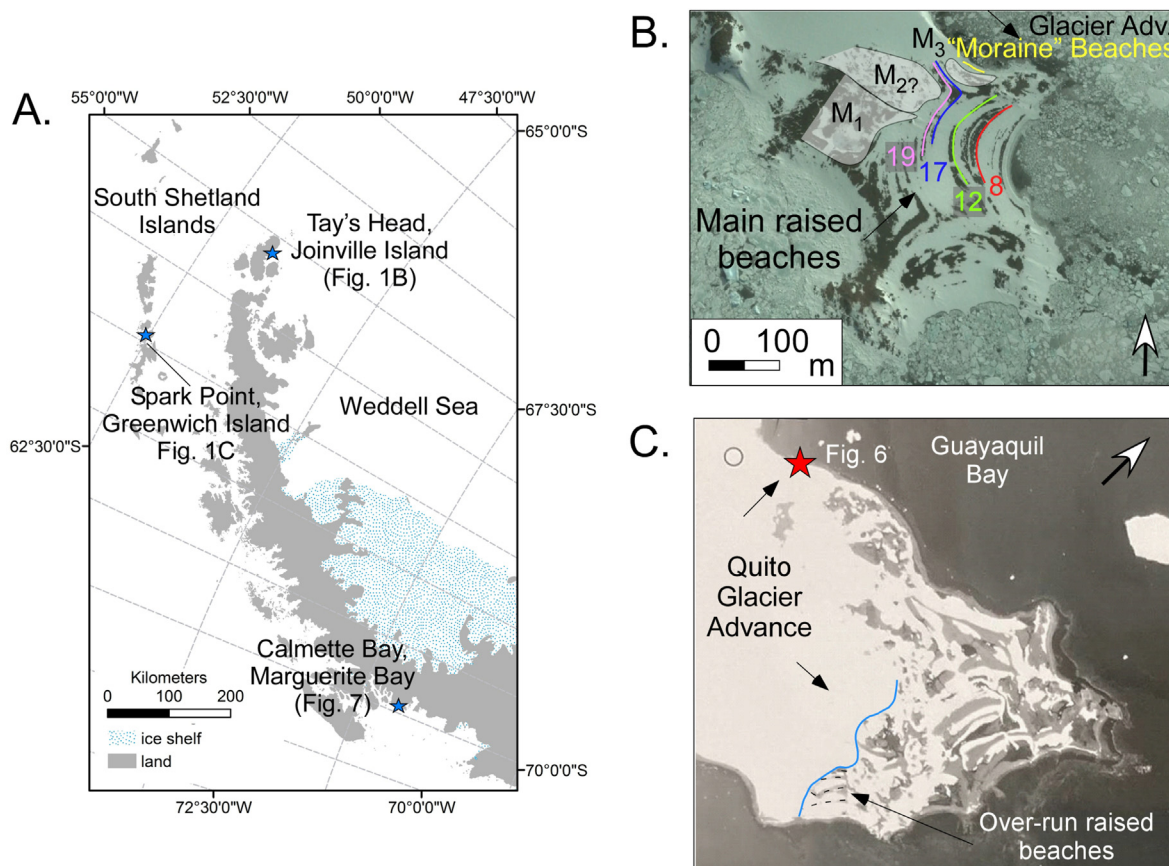


Fig. 1. A. Map of the study area showing the general location of the three study areas. B. Aerial photograph (GoogleEarth) of Tay Head on Joinville Island illustrating the features mentioned in the text. M₁, M₂, and M₃, represent potential Moraines 1–3, respectively. C. Aerial photograph of Spark Point illustrating the over-run raised beaches and the location of our new radiocarbon ages (Image taken 6 Jan. 1989). © Crown Copyright and/or database rights. Reproduced by permission of The Keeper of Public Records and the UK Hydrographic Office (www.GOV.uk/UKHO).

stable water isotopes identified the period between 1200 and 1900 CE (750–50 cal BP) as the coldest in the past 2000 years (Stenni et al., 2017). Contemporaneous reductions in snowfall are also observed in ice core reconstructions at continental (Frezzi et al., 2013) and regional scales (Thomas et al., 2017) and in surface mass balance simulated from climate models (Dalaiden et al., 2020). Evidence for cooler conditions as well as glacial or ice shelf expansion has been found in marine sedimentary records across Antarctica (Domack et al., 1995; Pudsey et al., 2006; Bentley et al., 2009; Simms et al., 2011b; Christ et al., 2015; Minzoni et al., 2015), but is notably absent in other marine records (Milliken et al., 2009; Michalchuk et al., 2009; Wolff et al., 2016). Terrestrial evidence for glacial expansion during the LIA across Antarctica is also fragmentary but increasing (Hall and Denton, 2002; Hall, 2007; Guglielmin et al., 2016). Within the Antarctic Peninsula, evidence for such an advance has been found on James Ross Island (Kaplan et al., 2020), the South Shetland Islands (Birkenmajer, 1979; Hall, 2007), and Marguerite Bay (Guglielmin et al., 2016). Proxy evidence for cooler conditions or locally expanded glaciers has also been found in several lake core (Bjorck et al., 1996) and moss-bank (Yu et al., 2016; Charman et al., 2018) records, but is notably absent in other terrestrial paleo-climate records (e.g. Sterken et al., 2012; Hodgson et al., 2013; Tavernier et al., 2014).

2.4. Raised beaches and glaciers

The non-cliffed ice-free coasts of the Antarctic Peninsula with

adequate sediment supply are host to several raised beaches formed largely in response to post-glacial rebound (John and Sugden, 1971; Curl, 1980; Fretwell et al., 2010). These raised beaches are generally found at higher elevations along the southern Antarctic Peninsula where in Marguerite Bay they reach elevations up to 40 m (e.g. Bentley et al., 2005; Simkins et al., 2013) than along the northern Antarctic Peninsula where Holocene raised beaches are generally found at elevations less than 20 m (Fretwell et al., 2010; Roberts et al., 2011; Zurbuchen and Simms, 2019). Due to their proximity to glaciers, high wave-energy, and the relatively high relief of the coastline, the beaches are generally coarse-grained with gravels and cobbles the most common grain sizes (Curl, 1980) and fine-grained coastal deposits are nearly absent across the region. Geomorphologically, these raised beaches generally come in two forms: strand plains and berm ridges (Lindhorst and Schutter, 2014). In more protected regions, the series of raised beaches is most commonly composed of either a continuous plain of prograding beach deposits or a suite of numerous low-relief raised beaches together referred to as strand plains (Lindhorst and Schutter, 2014). In more exposed reaches of the coast, the raised beaches are composed of fewer but higher-relief ridges with more aggradational and overwash characteristics as seen in ground-penetrating radar profiles (Lindhorst and Schutter, 2014). These are often referred to as berm ridges and are likely formed in response to large storms or periods of sediment starvation (Lindhorst and Schutter, 2014).

The early work by John and Sugden (1971) within the South

Shetland Islands was one of the first studies to systematically examine the relationship between raised beaches and moraines within the Antarctic Peninsula. A number of moraines were either cross-cut by or were themselves cross-cutting raised beaches (Sugden and John, 1973; Clapperton and Sugden, 1988). Before the advent of cosmogenic age dating techniques these cross-cutting relationships and lichenometry were among the few methods available to estimate the age of moraines within Antarctica. Clapperton and Sugden (1988) identified two phases of late Holocene moraines within the coves of Maxwell Bay on King George Island of the South Shetland Islands. The older “outer” moraines were younger than the 8.0- to 6.7-m beaches but older than the lower elevation 6-m beach while the younger “inner” moraines were younger than the 6-m beach. They suggested these two glacial advances dated to 1200–1500 CE and 1400–1600 CE, respectively (Clapperton and Sugden, 1988). Simms et al. (2012) used optically stimulated luminescence to refine the ages of those beach ridges suggesting that ice retreat following the most recent advance resulted in accelerated uplift of the islands. Based on their refinement of the beach ridge ages, the most recent moraine dates to 1500–1700 CE, roughly corresponding to the LIA in the northern hemisphere (Simms et al., 2012).

3. Methods

3.1. Raised beaches

Raised beaches at Joinville Island, Calmette Bay and Spark Point were surveyed using differential GPS (Fig. 1; Simkins et al., 2013; Fretwell et al., 2010; Zurbuchen and Simms, 2019). Within Joinville Island, the relationships between the moraines and beaches were mapped in the field. For Calmette Bay and Spark Point the cross-cutting relationships between the raised beaches and the local moraine or glacier were largely deduced from aerial photography although some of the relationships were noted during the field campaign to survey and date the raised beaches. All elevations reported for the beaches are with respect to mean sea level.

3.2. Dating

At Joinville Island, Simms and Zurbuchen (2019) found seaweed mats and limpet (*Nacellidae* sp.) shells imbedded within the raised-beach deposits. The seaweed appeared as mats interlaminated with the beach deposits and all 26 ^{14}C ages obtained by Zurbuchen and Simms (2019) were in stratigraphic order. In addition, limpet shells and seaweed from the same beaches returned the same calibrated ages within error (Zurbuchen and Simms, 2019). In this study we present four additional ^{14}C ages from limpets obtained from the raised beaches within the moraine mapped at Joinville Island (Table 1). AMS ages were run at the Keck Carbon Cycle AMS facility at the University of California Irvine. Two additional ^{14}C ages are provided on shells from a deposit at Spark Point. These ages were processed at the NERC Radiocarbon Laboratory in East Kilbride, UK (Table 1). All new radiocarbon ages are reported as calibrated years before present (cal BP) and were calibrated using Calib 8.2 (Stuiver et al., 2021), the MARINE20 calibration curve (Heaton et al., 2020), and a marine radiocarbon reservoir offset (ΔR) of 635 ± 42 based on the updated version of the Hall et al. (2010) reservoir corrected to the MARINE20 calibration curve (www.calib.org/marine/). The reservoir was applied to both shell and seaweed samples but not previously dated terrestrial mosses. Discussion continues on the appropriateness of the Hall et al. (2010) reservoir derived from the Ross Sea for applications in the Antarctic Peninsula; however, most other reservoir corrections suggested range between 1130 and 1424 years (e.g. Gordon and Harkness, 1992; Berkman and Forman, 1996)

and are within error of this reservoir when considering their errors of 100–200 years (see also Table 2). In addition, Simms et al. (2012) found good agreement to radiocarbon ages calibrated using the Hall et al. (2010) reservoir and OSL ages from the same beach elevations across King George Island within the South Shetland Islands of the Antarctic Peninsula. For previously dated mosses we use the SHCal20 calibration curve (Hogg et al., 2020).

Within Calmette Bay, raised beaches were dated by Simkins et al. (2013) using optically stimulated luminescence of cobble surfaces. Quartz aliquots were obtained by isolating the outer 1-mm of each buried cobble surface (Simms et al., 2011a; Simkins et al., 2013). Samples were gently crushed and sieved to isolate grains from 63 to 250 μm . Standard procedures were used subsequently, to prepare quartz separates. OSL measurements were conducted using a Risø TL/OSL-DA-15 Reader with blue stimulation and a U-340 detection filter. Equivalent doses were determined following the single-aliquot regenerative-dose (SAR) procedure (Murray and Wintle, 2000; Wintle and Murray, 2006). A detailed description of the procedure can be found in Simkins et al. (2013). We report OSL ages, as well as cosmogenic nuclide ages from earlier studies, as yrs BP.

4. Results

4.1. Joinville Island

Tay Head is a small ($\sim 2.5 \times 2.0$ km) ice-free peninsula extending into the Firth of Tay on the south side of Joinville Island. Its three seaward facing coasts contain a series of 36 raised beaches reaching an elevation of 13 m that are best developed on the east-facing shore of the peninsula. Most of the raised beaches exhibited seaward dipping reflections in ground-penetrating radar profiles characteristic of strand-plain deposits but three (ridges 2, 8, and 12) of the beach ridges were notably higher in relief than the others characteristic of the beach-berms of Lindhorst and Schutter (2014). Beach ridge 2 also exhibited landward-dipping reflections (Zurbuchen and Simms, 2019). Along its landward margin, the peninsula contains 2, possibly 3, sets of moraines or till sheets (Fig. 1B). The lowest and presumably youngest of these moraines or till sheets (moraine 3) is largely composed of a broad till sheet with a conspicuous sinuous-crested till ridge or esker (Fig. 2) cored by a matrix-supported diamicton (Fig. 3). The broad till sheet contains rounded pebbles and cobbles mixed with more angular clasts suggesting reworking of older beach deposits (Fig. 3). Inset into and seaward of moraine 3 are two additional raised beaches informally named “Upper Moraine Beach” and “Lower Moraine Beach”, which occur at elevations less than 2 m (Figs. 4 and 5). The till sheet and “Moraine Beaches” are separated from the main set of raised beaches dated by Zurbuchen and Simms (2019) by a paleo-tombolo and paleo sea stack (Figs. 1 and 5). Raised beaches 17 and 19 (beach 17 dates to 3095 ± 310 cal BP) occur at elevations of 5.8 and ~ 7.5 m asl, respectively, lie to the south of the paleo-tombolo, are continuous at an elevation above the paleo-tombolo, and are cross-cut by the younger till sheet (Fig. 5). Raised Beach 12 at an elevation of 4.3 m asl (dated to 2140 ± 310 cal BP and 2170 ± 320 cal BP; Table 1) is cut by the tombolo but a similar beach is found north of the tombolo at the same elevation as the dated beaches to the south of the tombolo (Fig. 5). A fourth more-ambiguous shore-parallel ridge, likely correlative with raised beach 8, occurs at an elevation of 3.7 m asl (dated to 1470 ± 170 and 1530 ± 170 cal BP; Table 1) and is found south of the tombolo. This beach is also found north of the tombolo and appears to be overrun by the till sheet. However, its marine origin and cross-cut relationship are less certain than those of the correlative raised beaches 17, 19, and 12.

Unlike the main beaches to the south of the tombolo, the

Table 1
New radiocarbon ages reported in this study.

Lab Number	Sample Number	Description	Material Dated	14C Age	Error (years)	Calibrated Age ^a (cal BP)	2σ Error (years)
<i>Zurbuchen and Simms (2019)</i>							
UCIAMS-208364	JVRC_01	Beach Ridge #1, Joinville Island	seaweed	980	15	modern	
UCIAMS-208209	JVRC_02	Beach Ridge #1, Joinville Island	Nacellidae sp.	1000	20	modern	
UCIAMS-208210	JVRC_09	Beach Ridge #3, Joinville Island	Nacellidae sp.	2065	20	810	150
UCIAMS-208637	JVRC_26-s	Beach Ridge #8, Joinville Island	seaweed	2710	20	1470	170
UCIAMS-208214	JVRC_26-l	Beach Ridge #8, Joinville Island	Nacellidae sp.	2755	20	1530	170
UCIAMS-208372	JVRC_39-s	Beach Ridge #12, Joinville Island	seaweed	3275	20	2160	180
UCIAMS-208215	JVRC_39-l	Beach Ridge #12, Joinville Island	Nacellidae sp.	3300	20	2190	190
UCIAMS-208388	JVRC_45	Beach Ridge #17, Joinville Island	seaweed	4060	15	3120	190
<i>This study</i>							
UCIAMS-208220	RC101-LMB	Upper Beach, Joinville Island	Nacellidae sp.	960	20	modern	
UCIAMS-208221	RC102-LMB	Upper Beach, Joinville Island	Nacellidae sp.	980	20	modern	
UCIAMS-208218	RC103-LMB	Lower Beach, Joinville Island	Nacellidae sp.	985	20	modern	
UCIAMS-208219	RC104-LMB	Lower Beach, Joinville Island	Nacellidae sp.	1035	20	modern	
SUERC-14419	SPA-SH01	Overrun beach, Spark Point, South Shetland Islands	<i>Laternula elliptica</i>	1552	37	370	160
SUERC-14420	SPA-SH02	Overrun beach, Spark Point, South Shetland Islands	<i>Laternula elliptica</i>	1557	37	380	160

^a Mean age of the 2σ range calibrated using Calib 8.2 (Stuiver et al., 2021) using the calibration curve MARINE20 and a marine radiocarbon reservoir ΔR of 635 ± 42 (Hall et al., 2010).

“Moraine Beaches” were not as stratified and lacked the seaweed mats prevalent in the main raised beaches (Fig. 4). However, we did find four limpet shells buried 10+ cm within the “Moraine Beaches.” Two radiocarbon ages obtained from the “Upper Moraine Beach” returned modern ages (Table 1). Two additional radiocarbon ages obtained from the “Lower Moraine Beach” also returned modern ages (Table 1). These four ages are nearly identical to the three ages returned from raised beaches 1 and 2 (also modern ¹⁴C ages) south of the tombolo (Zurbuchen and Simms, 2019). Taken together this suggests that the till sheet comprising Moraine 3 on Tay Head dates to less than 1500 cal BP and likely less than 810 ± 150 cal BP, which is the age of the youngest raised beach (beach 3; Table 1) that occurs outside of Moraine 3 but does not have a correlative beach inside Moraine 3, indicating that the beach is older than or correlative with the till sheet.

4.2. Spark Point

The headland of Spark Point constitutes a series of bedrock mesas surrounded by flights of raised beaches extending up to 16.16 m asl (Fretwell et al., 2010). Apart from the exposed headland most of the area is covered by the Quito Glacier, which flows into Guayaquil Bay on the north side of the headland with a second margin in the bay to the south of the headland (Fig. 1C). In both locations the ice margins reach the sea but in Guayaquil Bay the base of the glacier lies on a wave-cut platform exposed at low tide (Fig. 6). On the south side of the headland the raised beaches are overlain by the margin of the Quito Glacier (Fig. 1C). In Guayaquil Bay the glacier directly overlies a < 1 m thick sandy diamicton, which is massive in its lower part with stringers of silty material. This sandy diamicton is overlain by a fissile (deformed) diamicton. The lower part of the massive diamicton has abundant shells and shell

fragments, dominantly articulated paired valves of *Laternula elliptica* up to 8 cm in length, and an unidentified smaller (2–3 cm) species. The *L. elliptica* shells are well preserved with visible periostracum (outer) and nacre (inner pearly) layers (Fig. 6). The glacier-beach relationship and diamicton at Spark Point show that the Quito Glacier over-rode the beaches after deposition of an intertidal or sub-tidal sand deposit. Samples of the *L. elliptica* shells yield two similar ages of 370 ± 160 and 380 ± 160 cal BP (Table 1).

4.3. Calmette Bay

Calmette Bay is a small fjord within the northeastern portion of the larger Marguerite Bay of the southern Antarctic Peninsula (Fig. 1). Along its southern coastline is a well-developed set of raised beaches reaching an elevation of up to 40 m above sea level (Bentley et al., 2005; Hodgson et al., 2013; Simkins et al., 2013, Fig. 7). Based on OSL ages of rock surfaces, Simkins et al. (2013) found that the beaches lower than ~20 m elevation are Holocene in age while the beaches above 20 m elevation are likely late Pleistocene in age. Along the western edge of the beaches lies a glacial moraine (potentially ice-cored, with a second potentially older overrun moraine) that advanced over the raised beaches (Figs. 7 and 8). The lowest reliably dated raised beaches from Simkins et al. (2013) are from beaches 3 and 5, which occur at elevations of 3.3 and 3.4 m, respectively. Two OSL ages were obtained from beach 3 of 1000 ± 300 and 730 ± 240 yrs BP, yielding a weighted mean of 835 ± 187 yrs BP. Two additional OSL ages were obtained from beach 5 of 2560 ± 510 and 2980 ± 280 yrs BP, yielding a weighted mean age of 2885 ± 245 yrs BP. Farther to the west of our sample sites, several additional beach ridges younger than beach 3 of Simkins et al. (2013) are cut by the moraine, suggesting an advance of the glacier well after 835 ± 187 yrs BP.

Table 2
Summary of existing evidence for LIA cooling or glacial or ice-shelf advance across the Antarctic Peninsula over the last ~1200 years.

Reference	Map ^b	Type of Indicator	Included in OxCal Model	Location	Originally Reported Timing of LIA conditions	Comments	Originally reported ¹⁴ C age (yrs)	Error (yrs)	Mean Recalibrated Ages (Cal yrs BP) ^a	Error (yrs)	Relationship between original ¹⁴ C age and LIA indicator
Yoo et al. (2009)	1	MP	N	northern South Shetland Shelf	1620 AD (330 cal BP)	Used coretop age (2600 yrs) to calibrate	NA				
Yoon et al. (2010)	2	MP	N*	Maxwell Bay (South Shetland Islands)	1310 AD (640 ± 55 cal BP)	1300 14C reservoir applied	1719	55	520 ^b	180	Age within the LIA deposit
Hass et al. (2010)	3	MP	N*	Maxwell Bay (South Shetland Islands)	1400–1900 AD (550–50 cal BP)	1100 14C reservoir applied	1660 & 1800	25	470 ^b & 580 ^b	160 & 120	Age within the LIA deposit
Majewski et al. (2012)	4	MP	Y	Maxwell Bay	1450–1950 AD (<500 cal BP)	1100 14C reservoir applied	1495	15	330 ^b	170	LIA younger than this age (Maximum age)
Hall (2007)	5	TA	Y	Colins Ice Cap (SSI)	post 1340 AD (<610 cal BP)	terrestrial mosses reworked into moraine	677	45	605	60	LIA younger than this age (Youngest incorporated age)
Birkenmajer (1979)	6	TA	Y	King George Island (SSI)	1720 AD	Lichenometry	NA				Age of the LIA moraine
Clapperton and Sugden (1988)	7	TA	N	South Shetland Islands	1200–1500 AD; 1400–1600 AD	Based on compilation of ages	NA				Age of the LIA
This Study	A	TA	Y	Spark Point, South Shetland Islands	Post 1730 (<220 cal BP)	beach overrun by moraine	1552 & 1557	37 & 37	370 ^b & 380 ^b	160 & 160	LIA younger than this age (Maximum age)
Curl (1980)	8	TA	Y	Livingston Island (SSI)	1700 AD	Lichenometry	NA				Age of the LIA moraine
Khim et al. (2002)	9	MP	N	Bransfield Basin	1500–1950 AD (450–0 cal BP)	Used coretop age (3000 years) to calibrate	NA				
This Study	B	TA	Y	Joinville Island	Post 1255 AD (<695 cal BP)	beaches overrun by moraine	2065	20	810 ^b	150	LIA younger than this age (Maximum age)
Minzoni et al. (2015)	10	MP	Y	Herbert Sound (James Ross Island)	1570 AD (380 cal BP)	1100 14C reservoir applied	1505	30	340 ^b	180	LIA younger than this age (Maximum age)
Kaplan et al. (2020)	11	TA	Y	James Ross Island	1740 AD (210 ± 45 yrs BP)	Average of 8 10Be ages	NA				Age of the LIA moraine
Pudsey et al. (2006)	12	ISA	Y	Prince Gustav Channel (Larsen)	Pre-1902	Based on historical accounts	NA				LIA older than this age (Minimum age)
Charman et al. (2018)	13	TP	N	Across northern AP	1450–1850 AD (500–100 cal BP)	Records binned at 100 year time intervals	NA				Age of the LIA
Domack et al. (1995)	14	ISA	Y	Muller Ice Shelf (Lallemand Fjord)	1550 AD (400 cal BP)	Used coretop age to calibrate	1945	85	710 ^b	210	LIA younger than this age (single foram date, rest are organic dates)
Yu et al. (2016)	15	TA	Y	Near Anvers Island	1190–1350 AD (760–600 cal BP)	Terrestrial mosses overrun by ice	685	25	610	50	LIA younger than this age (Youngest overridden age)
Smith (1982)	16	TA	Y	Anvers Island	post 1595 AD (<425 cal BP)	Terrestrial mosses overrun by ice	425	40	415	90	LIA younger than this age (Youngest overridden age)
Leventer et al. (1996)	17	MP	N	Palmer Deep	1450–1650 AD (500–300 cal BP)	Used coretop age (2200) to calibrate	NA				
Domack et al. (2001)	18	MP	Y	Palmer Deep	1250–1850 AD (700–100 cal BP)	1230 14C reservoir applied	2200	50	960 ^b	200	LIA younger than this age (Maximum age)
Shevenell and Kennett (2002)	19	MP	Y*	Palmer Deep	1250–1750 AD (700–200 cal BP)	Same age model “ as Domack et al. (2001)		“			“
Shevenell et al. (2011)	20	MP	Y*	Palmer Deep	1500–1800 AD (500–200 cal BP)	Same age model “ as Domack et al. (2001)		“			“
Kim et al. (2018)	21	MP	N*	Bigo Bay (WAP)	1270–1670 (680–280 cal BP)		1660	30	470 ^b	160	Age within the LIA deposit

Table 2 (continued)

Reference	Map ^b	Type of Indicator	Included in OxCal Model	Location	Originally Reported Timing of LIA conditions	Comments	Originally reported ¹⁴ C age (yrs)	Error (yrs)	Mean Recalibrated Ages (Cal yrs BP) ^a	Error (yrs)	Relationship between original ¹⁴ C age and LIA indicator
Christ et al. (2015)	22	MA	Y	Barilari Bay (WAP)	Pre-1700 (>250 cal BP)	1390 14C reservoir applied	1600	25	410 ^b	140	LIA older than this age (Minimum age)
Christ et al. (2015)	23	ISA	Y	Barilari Bay (WAP)	1220–1870 AD (730-82 cal BP)	1390 14C reservoir applied	2180	35	930 ^b	180	LIA Younger than this age (age from base of unit with other younger ages in the unit)
This Study	C	TA	Y	Calmette Bay (Marguerite Bay)	Post 1175 AD (<835 ± 187 yrs BP)	beaches overrun by moraine	NA				
Guglielmin et al. (2016)	24	TA	Y	Rothera Point	1280-1630+ AD (671–317+ cal BP)	terrestrial mosses	710	40	615	60	LIA younger than this age (most landward overridden age)

N*: these ages were originally included but returned A values of less than 60 in the OxCal model, thus treated as outliers in the final age model (their inclusion resulted in <50 year difference in the age model).

Y*: Used the same age model as Domack et al. (2001) so only included once in the OxCal model as not to replicate the same original age constraint.

^a Calibrated using SoCal20 (Hogg et al., 2020) unless marked; Ages used for Fig. 9, not the OxCal model.

^b Calibrated using MARINE20 and a radiocarbon reservoir offset (ΔR) of 635 ± 42.

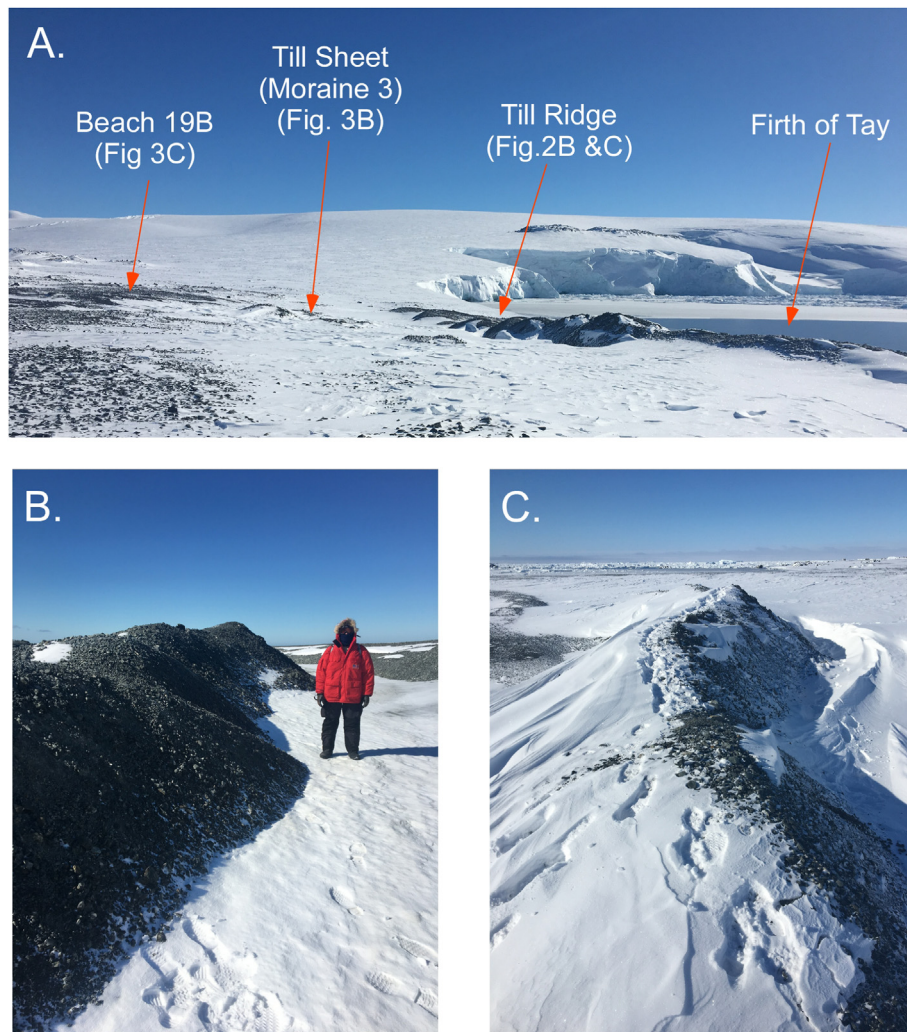


Fig. 2. Photographs of the till ridge at Tays Head, Joinville Island (B and C) as well as the spatial relationship between the till ridge, Beach 19B, and the ocean (Firth of Tay) (A). See Fig. 1 for general location.

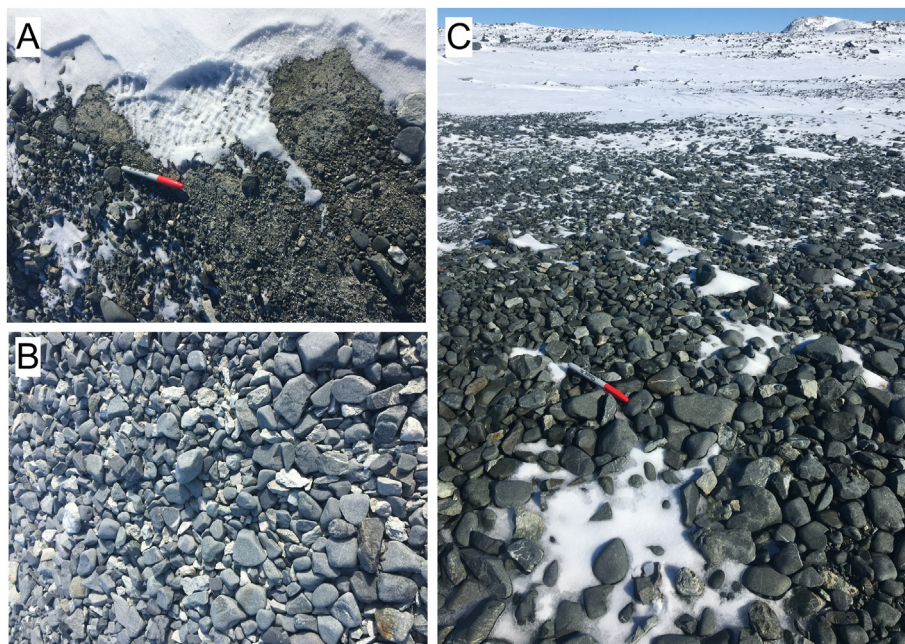


Fig. 3. Photographs of A) diamicton within the till ridge, B) reworked beach cobbles in moraine 3, and C) beach cobbles in beach 19B landward of the till ridge of moraine 3 at Tays Head, Joinville Island. See Fig. 1 for general location.

5. Discussion

5.1. Timing of glacial advance

The available constraints from both Joinville Island and Calmette Bay suggest the most recent glacial advance in these locations occurred more recently than ~800 cal BP. The ages from Spark Point suggests an advance occurred there more recently than ~380 cal BP. These two advances may represent the same event as the ages from Joinville Island and Calmette Bay are minimum ages. However, given the age uncertainties, it is possible that the Joinville and Calmette Bay advances pre-dated the advance at Spark Point. Evidence for two glacial advances in the South Shetland Islands within the last 1 ka was presented by Clapperton and Sugden (1988) and is considered later. Regardless of the potential variability in timing among these three advances, all appear to have occurred during the time of the Northern Hemisphere LIA suggesting that LIA advances occurred in the Antarctic Peninsula.

5.2. Comparison with other records and timing of the LIA in the Antarctic Peninsula

This study is not the first to provide ages of glacial expansion across the Antarctic Peninsula consistent with the timing of the LIA within the Northern Hemisphere (Table 2; Fig. 9). Birkenmajer (1979); Curl (1980), Clapperton and Sugden (1988), and Simms et al. (2012) each suggested the most recent advance within the South Shetland Islands occurred at the same time as the LIA in Europe. Hall (2007) provided more data to refine the timing of the event within the South Shetland Islands with a detailed study of moraines outboard of the Collins Ice Cap on King George Island. Using mosses reworked into the moraine she found that the advance of the ice occurred within the last ~600 years. Similar studies from Anvers and Adelaide Islands by Yu et al. (2016) and Guglielmin et al. (2016), respectively, came to similar conclusions. In a recent study that used cosmogenic ages to determine the age of glacial landforms across James Ross Island, Kaplan et al. (2020)

obtained four ^{10}Be ages from a series of frontal moraines within Rhum Cove and an additional four ^{10}Be ages from Croft Bay, suggesting an advance within the last 300 years. Based on these and a number of other records (Table 2, Figs. 9 and 10), it appears a LIA advance and possible cooling was widespread throughout the Antarctic Peninsula from 450 to 150 cal BP (Figs. 9 and 10). Thus, the LIA advances we report here do not appear to be localized glacier advances but instead are representative of a more regional-scale event.

The one record that appears to show cooling at a different period is the ice-core record from the EAP at James Ross Island (JRI), which shows cooling but at a time (800–400 yr BP) preceding that from most other records across the Antarctic Peninsula (Mulvaney et al., 2012). However, the 2000-year temperature anomaly from the JRI ice core is poorly correlated with northern hemisphere temperature reconstructions, suggesting that the stable water isotope record from this site may not be a suitable indicator of LIA associated cooling. This discrepancy may reflect differences across the EAP and WAP, as most of the evidence for a LIA are from the WAP (Fig. 9). Alternatively, the maritime location of JRI, in the shadow of the Antarctic Peninsula, may be capturing local rather than regional changes (Abram et al., 2011) sensitive to local sea ice conditions and extreme precipitation events (Turner et al., 2019). A more consistent cooling trend is observed between ~1700 and 1900 CE (250–50 yr BP) in the other stable water isotope records from the Antarctic Peninsula, despite evidence that high-frequency processes influence the variability (Thomas and Tetzner, 2018). At the continent-wide scale, the composite from Stenni et al. (2017) suggest a period of persistent cold anomalies between ~1200 and 1900 CE (750–50 yr BP). An equally coherent pattern is observed in the snow accumulation records from this region, with consistently lower snowfall between ~1700 and 1900 CE (250–50 yr BP; Thomas et al., 2015; Thomas and Tetzner, 2018). Recent evaluation using climate models has indicated that snow accumulation may be a better proxy for past surface temperature than stable water isotopes (Dalaiden et al., 2020; Cavitte et al., 2020); however, the snow accumulation record for JRI is not available. Surface mass balance

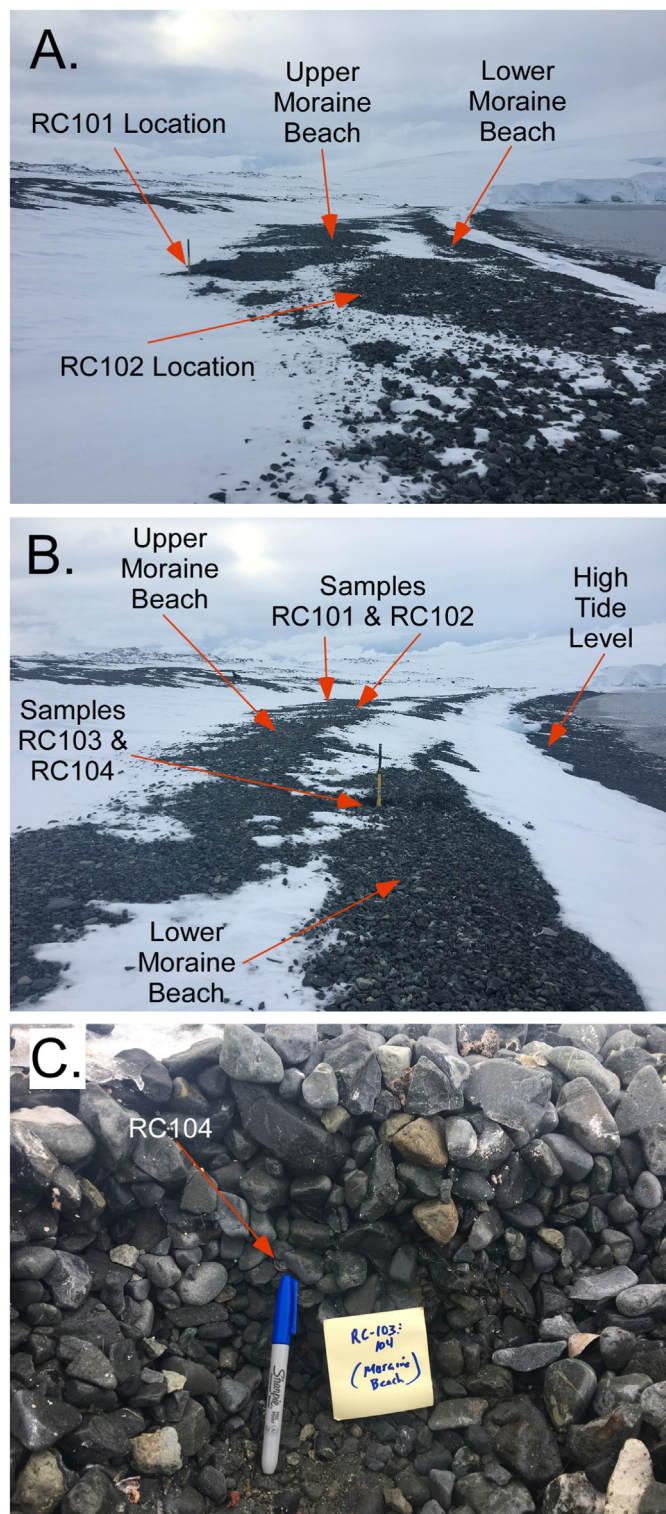


Fig. 4. Photographs of the “Upper” and “Lower Moraine Beaches” at Tays Head, Joinville Island (A and B) as well as the character of their deposits (C). See Fig. 1 for general location.

(snow accumulation) simulated in global circulation models spanning the past millennium indicate that snowfall in West Antarctica was lowest during the LIA (Dalaiden et al., 2020).

Suggestions for a dipole in climate across the EAP and WAP are still a matter of discussion (Charman et al., 2018). While our new record from Joinville Island on the EAP could fit with the timing of Mulvaney et al. (2012), as it limits the LIA advance on Joinville Island to within the last 800 years, Kaplan et al. (2020) provides compelling evidence for a glacial advance 210 ± 45 yrs BP from moraines on James Ross Island, the same island as the ice core). Potentially the expansion seen on the EAP is driven by lower rates of ablation or higher rates of precipitation rather than cooler temperatures. Unfortunately, the other records of cooling or ice advance on the EAP (Minzoni et al., 2015; Pudsey et al., 2006) do not provide conclusive evidence either way. The LIA signal recorded by Minzoni et al. (2015) is muted but later (recalibrated to $<340 \pm 180$ cal BP from the originally reported ~ 380 cal BP), while the record of Pudsey et al. (2006) is only loosely constrained temporally due to the very large core-top age.

We combined our new age constraints on the LIA with other records of LIA advances or cooling to estimate the age of the LIA across the Antarctica Peninsula (Table 2). We did not include those records shown in Fig. 9 in which a coretop age was used to correct the ^{14}C ages (largely from cores dated using acid-insoluble organic ages) or composites of ages where the particular ages used were uncertain (e.g. Clapperton and Sugden, 1988). We conducted this analysis using the Bayesian age modeling program OxCal 4.4 (Bronk Ramsey, 2009) with the MARINE20 curve (Heaton et al., 2020) and the ΔR value of Hall et al. (2010) (corrected to the MARINE20 curve) for all marine samples and the SHCal20 curve of Hogg et al. (2020) for the terrestrial moss samples. In our initial simple model, we express these constraints as three “phases” separated by two “boundaries.” The first phase represents all the chronological constraints obtained from either deposits below the beds representing the LIA or material reworked into LIA moraines, while the second phase represents all ages taken from the LIA indicator beds themselves or direct ages from the moraines (e.g. cosmogenic ages or lichenometry ages). The third phase represents all ages from beds deposited after the LIA evidence. The boundaries between these phases thus represent the beginning and ending of the LIA within the Antarctic Peninsula. Based on this output, we arrive at a beginning of the LIA within the Antarctic Peninsula of 310 cal BP (400–210 cal BP; 95%) or 1640 CE (1550–1740 CE) and an end of 190 cal BP (290–90 cal BP; 95%) or 1760 CE (1660–1860 CE) (see Supplementary Fig. 1), which when combined gives an age range of 400 to 90 cal BP (1550–1860 CE). This result includes four ages without an A value, a metric for fit in Oxcal, > 60 , which were treated as outliers in the final OxCal model (Table 2). Including them in the Oxcal analysis gave slightly older ages (360–220 cal BP) but still within error of the age assignment when excluding the outliers; however, this solution produces total A values much lower than the typical acceptance criteria of $A > 60$. As Clapperton and Sugden (1988) do find evidence of two separate advances in the South Shetland Islands and two moraines of this approximate age may be present at Calmette Bay (Fig. 7), we also considered a Bayesian age model in which the ages are grouped into two advances represented by “phases” separated by the youngest pre-LIA ages denoted as a separate phase (see Supplementary Fig. 2). Doing

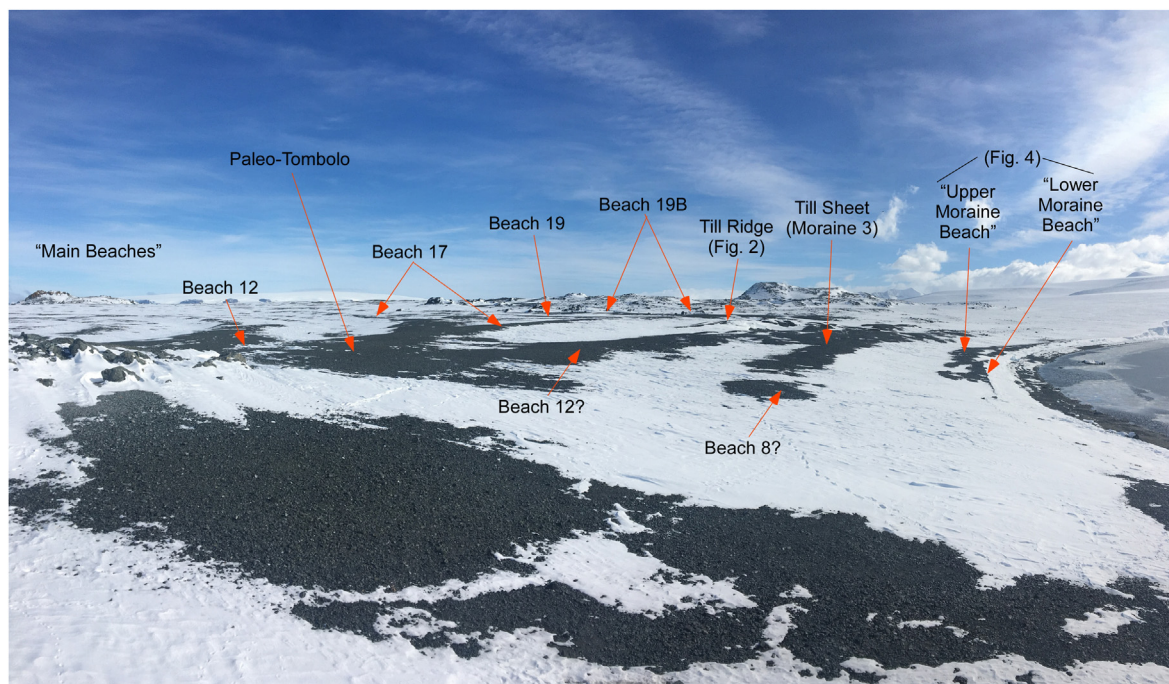


Fig. 5. Panorama photograph illustrating the spatial and cross-cutting relationships of the beaches and moraine 3 at Tays Head, Joinville Island. See Fig. 1 for general location.

this required only one outlier (the older of the two Hall et al., 2010 ages) within the age model and gave A values comparable to that of the single LIA phase when removing the outliers (overall A-values of 109.4 versus 114.3 for the model removing the 4 outliers). Such a two phase advance might reconcile the apparently conflicting timing of the LIA in ice cores with each other (both that of Mulvaney et al., 2012 and Thompson et al., 1994) and our compilations as well as providing support for Clapperton and Sugden (1988) findings of two advances. However, we stress that our suggestion of a two-phase glacial advance is based solely on age distributions and other than the Clapperton and Sugden (1988) study and the possible second moraine at Calmette Bay, definitive evidence for two separate advances has yet to be identified. Further work is needed to determine if the LIA was marked by two advances within the Antarctic Peninsula.

5.3. Implications for LIA forcings

Because the glacial advances occur at the same time indicated by cooling within many climate proxy records across the Antarctic Peninsula (Table 2; Fig. 10), it appears cooling drove the advance rather than precipitation during a warmer period. Available records of snow accumulation from the Antarctic Peninsula extending beyond ~150 yr BP (1800 CE) are limited (Thomas et al., 2017). However, the available records dating back to the period immediately after the LIA show an increase, rather than a decrease, in snow accumulation (and thus by extension precipitation) since ~150 yr BP (Thomas et al., 2017). This is further supported by ice cores from coastal Ellsworth Land, which show a strong regional coherence with precipitation on the Antarctic Peninsula. These sites provide evidence for a prolonged period of low snow accumulation and stable conditions between ~1700 and 1900 CE (250–50 yr BP;

Thomas et al., 2015). Farther to the East within the Transantarctic Mountains, Bertler et al. (2011) found evidence for cooler and drier conditions during the LIA based on ice-core records. As the timing of the advances is coincident with those of the Northern Hemisphere, it would support assertions of a volcanic driver for the LIA (Miller et al., 2012; Porter et al., 2021). A recent reconstruction of the Interdecadal Pacific Oscillation (IPO), based on ice cores from the Antarctic Peninsula, suggested that the LIA was dominated by a negative IPO state (Porter et al., 2021) and hence more La Niña-like conditions. While they find no correlation between the IPO and volcanic forcing, they note that the dynamical relationships with the intertropical convergence zone, evident during the rest of the record, is absent during the LIA. The Antarctic Peninsula's climate may be largely driven by Pacific teleconnections (e.g., Pike et al., 2013), such as the Southern Annular Mode (Thomas et al., 2008), and SST anomalies in the western Pacific (Thomas et al., 2008, 2015). Thus, records from the Antarctic Peninsula may not reflect the climate of Antarctica as a whole (Charman et al., 2018). However, the LIA-advance is also found on the EAP (Joinville Island and Kaplan et al., 2020), which although still a matter of discussion (e.g. Charman et al., 2018), is largely governed by Weddell Sea climate interactions (Reynolds, 1981; Barbara et al., 2016) and thus the LIA event may be reflective of a larger event throughout Antarctica. Ice core records from other parts of West Antarctica do show cooling during this time period (Orsi et al., 2012), although LIA glacial advances in that sector of Antarctica have yet to be documented. Across portions of East Antarctica, colder conditions have been documented in the Ross Sea sector (Bertler et al., 2011; Rhodes et al., 2012) along with local glacial expansion (e.g. Baroni and Orombelli, 1994; Hall and Denton, 2002). Further to the east however, evidence for a LIA-like glacial advance has yet to be found. Several records even point to warmer periods during this time

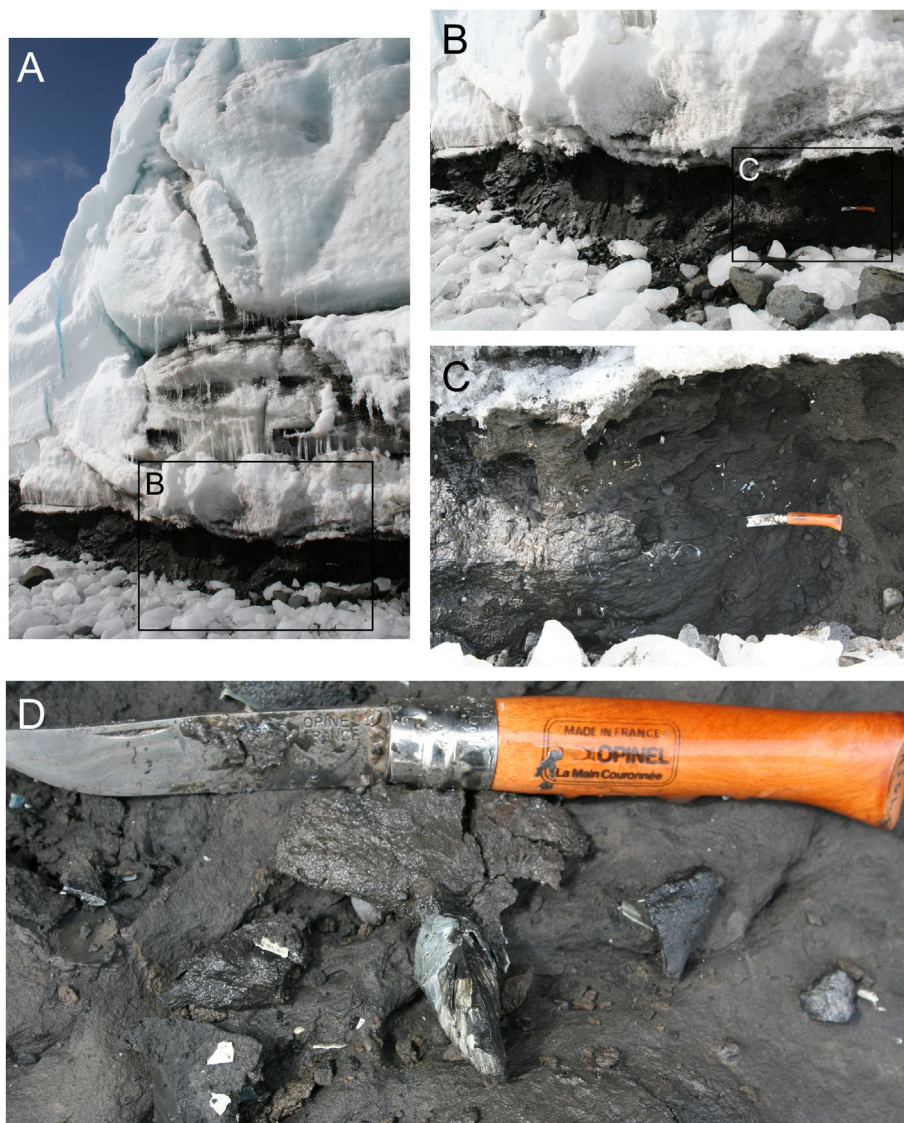


Fig. 6. Photographs illustrating the terminus of the Quito glacier into Guayaquil Bay at Spark Point and its relationship with the marine deposits it overran (A–C). D.) Photograph of one of the *L. elliptica* shells dated as part of this study. See Fig. 1 for general location.

across coastal portions of the Indian Ocean sector of East Antarctica (Tavernier et al., 2014). More work is warranted to determine the spatial extent of the LIA across other portions of Antarctica.

5.4. Implications for RSL and glacial-isostatic adjustment models

Recognition of a weak Earth structure beneath the Antarctic Peninsula (Nield et al., 2014; Simms et al., 2012, Simms et al., 2018) and West Antarctic in general (Barletta et al., 2018) is growing. In addition, several studies have argued that the Holocene fall in RSL around portions of West Antarctica may not necessarily reflect rebound from the retreat of ice from the Last Glacial Maximum but may be strongly controlled by late Holocene glacial advances (and retreats) (e.g. Ivins and James, 2005; Simms et al., 2018; Kingslake et al., 2018; Zurbuchen and Simms, 2019). Our new data provides evidence for the late Holocene glacial oscillations that might have

driven these late Holocene RSL changes and “masking” of the Last Glacial Maximum signal in RSL records across the Antarctic Peninsula. Thus, the missing ice (e.g. (Simms et al., 2019)) at the Last Glacial Maximum may be “hiding” within Antarctica.

6. Conclusions

We identified glacial moraines representing a recent glacial advance that occurred within the last ~800 years and possibly as recently as 370 cal BP at three locations across the Antarctic Peninsula. At Tay Head on Joinville Island a moraine cross-cuts raised beaches younger than ~1500 cal BP, possibly as young as 810 ± 150 cal BP with only modern beach ridges developed inside the moraine. At Calmette Bay within Marguerite Bay, raised beaches as young as 835 ± 137 yrs BP are cut by a glacial moraine. At Spark Point within the South Shetland Islands a moraine overrides

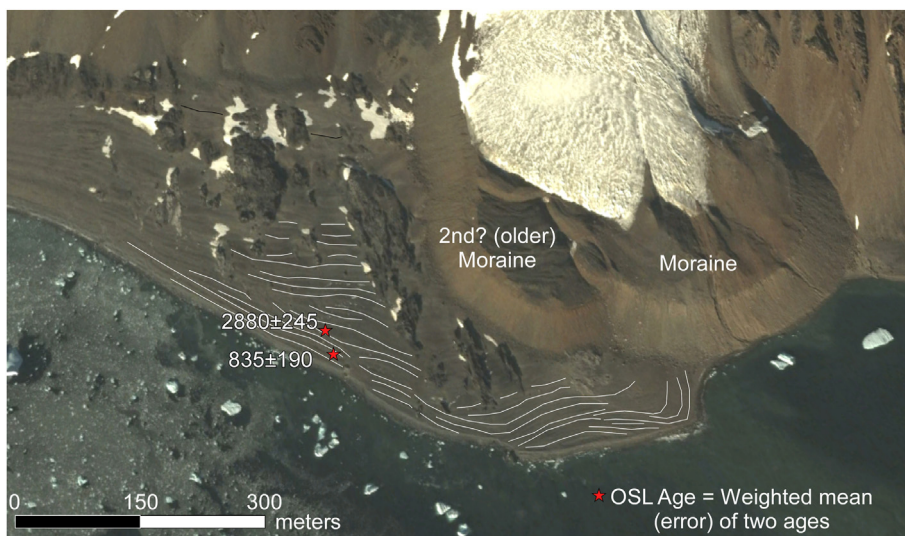


Fig. 7. Satellite image from Google Earth illustrating the cross-cutting relationship between a Little Ice Age moraine and raised beaches dated by Simkins et al. (2013) at Calmette Bay. See Fig. 1 for general location.

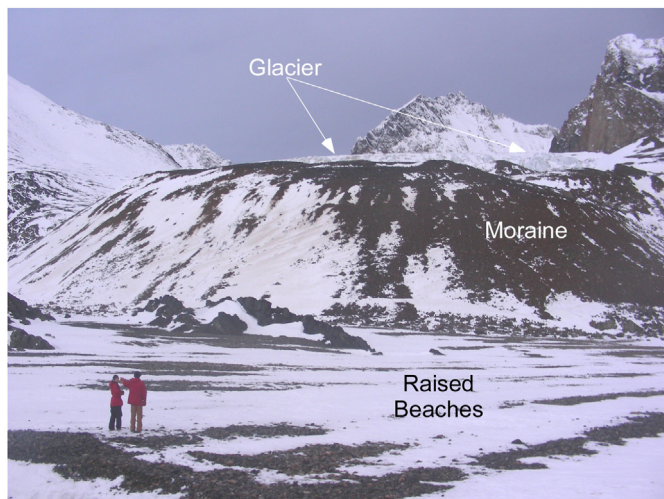


Fig. 8. Photograph of the moraine and raised beaches at Calmette Bay.

marine deposits with shells as young as 370 cal BP. These new ages are in agreement with other records of both glacial advances and cooler conditions from across the Antarctic Peninsula that when combined into a Bayesian framework suggest the LIA in the Antarctic Peninsula occurred between 400 cal BP and 90 cal BP (1550–1860 CE; 95%) and may have been represented by two separate advances. Its widespread identification suggests that the recent glacial advances indicated in this work represent not only local advances but are part of a larger climatic pattern experienced across the region. The available age constraints suggest that the cool period and glacial advances were largely contemporaneous with the LIA documented across many other parts of the globe. The apparent synchronicity of these conditions throughout the world supports recent assertions of a volcanic or solar driver for the LIA.

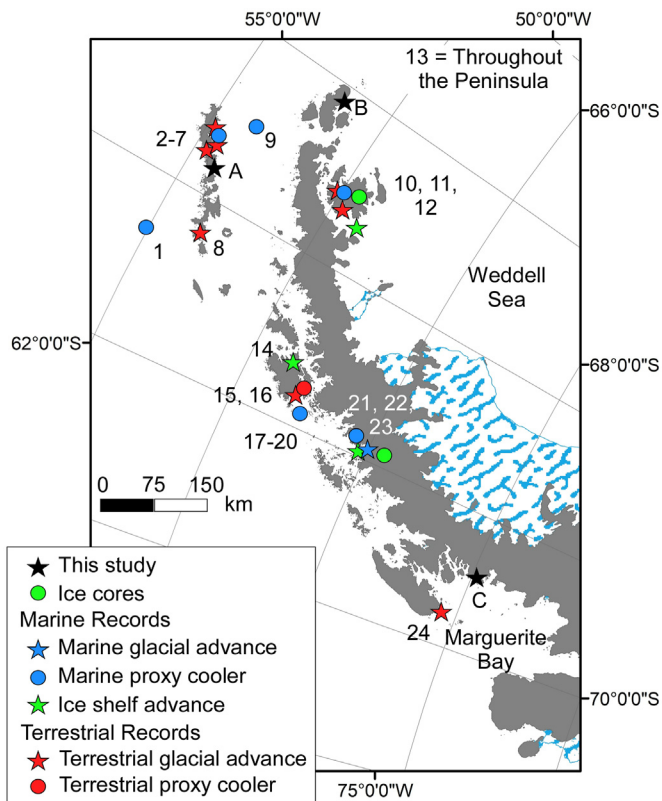


Fig. 9. Summary map showing locations of this study (black stars), ice cores discussed (green circles), and other studies that have found evidence for cooler conditions (blue and red circles), ice shelf growth (green stars), or glacial advances (blue and red stars) during the time period of the Little Ice Age. (For interpretation of the references to colour in this figure legend, the reader is referred to the Web version of this article.)

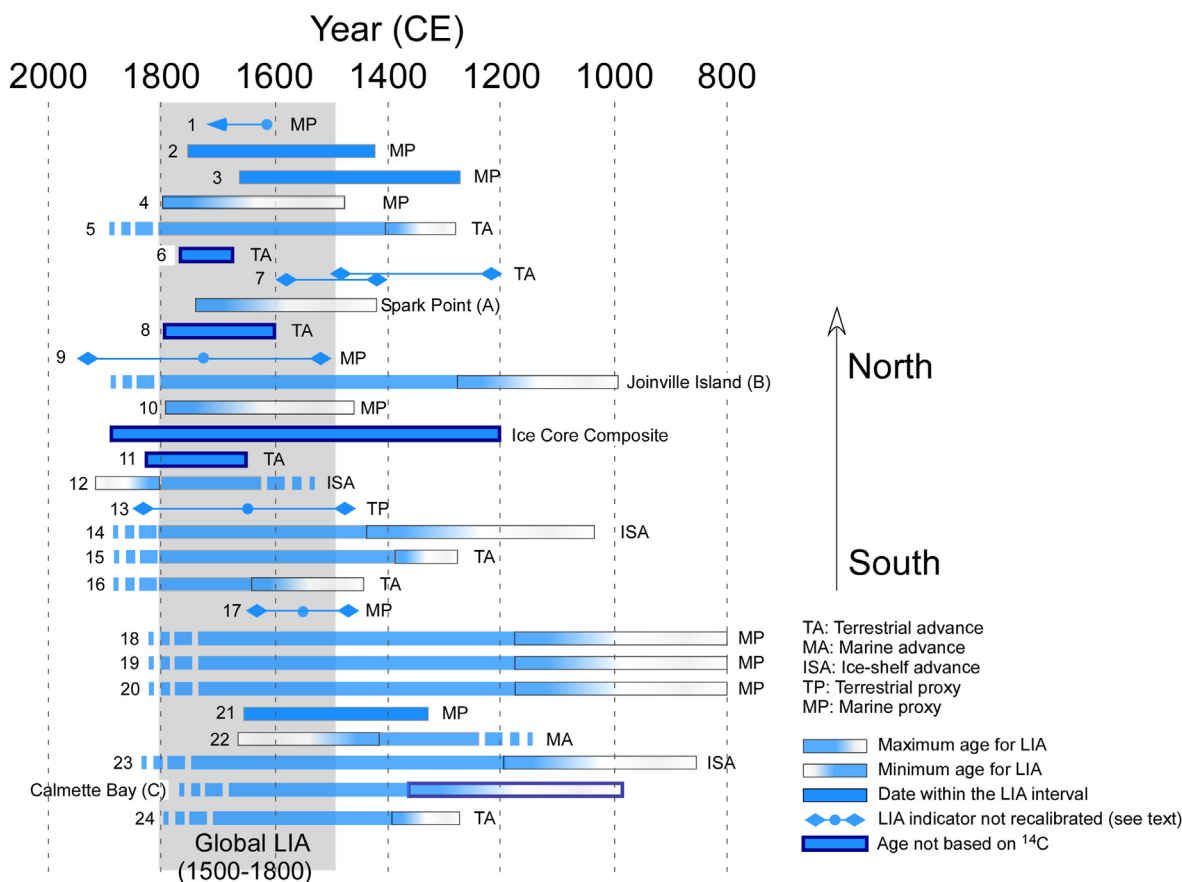


Fig. 10. Summary timeline of evidence of glacial advance or cooler conditions across the Antarctic Peninsula over the last 1200 years ordered from north (top) to south (bottom).

Author contributions

ARS designed the experiment. ARS, MB, LR, JZ, and LS conducted fieldwork. ARS and JZ conducting the radiocarbon age analysis while LS and RD conducted the OSL analysis. ET helped place the ages into a larger climatic framework. ARS conducted the OxCal modeling. ARS wrote the manuscript with input from MB, LR, LS, ET, and the rest of the authors.

Declaration of competing interest

The authors declare that they have no known competing financial interests or personal relationships that could have appeared to influence the work reported in this paper.

Acknowledgements

This work was funded in part by the National Science Foundation Office of Polar Programs through awards 1644197 and 0838781. We also thank Chris Denker, Cara Ferrier, Daniel Livsey, Chris Garcia, and the Captains and Crews of the R/V Nathaniel B. Palmer, R/V Laurence M. Gould, and the ARA Almirante Irizar for their help in the field. We also thank John Southon and Chanda Bertrand for their help with ¹⁴C dating at the University of California Irvine's W.M. Keck Carbon Cycle Accelerator Mass Spectrometer and Eric Benton for the gamma spectrometry measurements. The Spark Point data were collected by M.B. as part of a contribution to the British Antarctic Survey programme GRADES-QWAD, and we are grateful to the crew and pilots of HMS *Endurance* and field operations team at British Antarctic Survey for

their support of the work. We thank the NERC Radiocarbon laboratory for the Spark Point ages, which were provided as part of allocation no. 15.7001 to M.B. The authors acknowledge PALSEA, a working group of the International Union for Quaternary Sciences (INQUA) and Past Global Changes (PAGES), which in turn received support from the Swiss Academy of Sciences and the Chinese Academy of Sciences. This research is a contribution to the SCAR SERCE program. We thank reviewers David Sugden and an additional anonymous reviewer for their beneficial comments.

Appendix A. Supplementary data

Supplementary data to this article can be found online at <https://doi.org/10.1016/j.quascirev.2021.107195>.

References

Abram, N.J., Mulvaney, R., Arrowsmith, C., 2011. Environmental signals in a highly resolved ice core from James Ross Island, Antarctica. *J. Geophys. Res.* 116, D20116. <https://doi.org/10.1029/2011JD016147>.
 Anderson, J.B., 1999. *Antarctic Marine Geology*. Cambridge University Press, New York, NY.
 Barbara, L., Crosta, X., Leventer, A., Schmidt, S., Etourneau, J., Domack, E.W., Masse, G., 2016. Environmental responses of the northeast Antarctic Peninsula to Holocene climate variability. *Paleoceanography* 31, 131–147.
 Barletta, V.R., Bevis, M., Smith, B.E., Wilson, T., Brown, A., Bordoni, A., Willis, M., Khan, S.A., Rovira-Navarro, M., Dalziel, I., Smalley, R.J., Kendrick, E., Konfal, S., Caccamise, D.J.I., Aster, R.C., Nyblade, A., Wiens, D.A., 2018. Observed rapid bedrock uplift in Amundsen Sea Embayment promotes ice-sheet stability. *Science* 360.
 Baroni, C., Orombelli, G., 1994. Holocene glacier variations in the terra nova bay area (Victoria land, Antarctica). *Antarct. Sci.* 6, 497–505.
 Bentley, M.J., Hodgson, D.A., Sugden, D.E., Roberts, S.J., Smith, J.A., Leng, M.J., Bryant, C., 2005. Early Holocene retreat of the George VI ice shelf Antarctic

- peninsula. *Geology* 33, 173–176.
- Bentley, M.J., Hodgson, D.A., Smith, J.A., O Cofaigh, C., Domack, E.W., Larter, R.D., Roberts, S.J., Leventer, A., Hjort, C., Hillenbrand, C.D., Evans, D.J.A., 2009. Mechanisms of Holocene palaeoenvironmental change in the Antarctic peninsula. *Holocene* 19, 51–69.
- Bentley, M.J., Johnson, J.S., Hodgson, D.A., Dunai, T., Freeman, S.P.H.T., O Cofaigh, C., 2011. Rapid deglaciation of Marguerite bay, western Antarctic peninsula in the early Holocene. *Quat. Sci. Rev.* 30, 3338–3349.
- Berkman, Paul A., Forman, Steven L., 1996. Pre-bomb radiocarbon and the reservoir correction for calcareous marine species in the Southern Ocean. *Geophys. Res. Lett.* 23, 363–366.
- Bertler, N.A.N., Mayewski, P.A., Carter, L., 2011. Cold conditions in Antarctica during the Little Ice Age - implications for abrupt climate change mechanisms. *Earth Planet Sci. Lett.* 308, 41–51.
- Birkenmajer, K., 1979. Lichenometric dating of glacier retreat at Admiralty bay, king George island (South Shetland islands, west Antarctica). *Bull. Pol. Acad. Sci. Earth Sci.* 27, 77–85.
- Björck, S., Ingólfsson, O., Zale, R., Ising, J., 1996. Holocene deglaciation chronology from lake sediments. In: Lopez-Martinez, J., Thomson, M.R.A., Arche, A., Björck, S., Ellis-Evans, J.C., Hathway, B., Hernandez-Cifuentes, F., Hjort, C., Ingólfsson, O., Ising, J., Lomas, S., Martinez De Pison, E., Serrano, E., Zale, R., King, S. (Eds.), *Geomorphic Map of Byers Peninsula, Livingston Island*. British Antarctic Survey, Cambridge, UK, pp. 49–55.
- Bradley, R.S., Jones, P.D., 1993. 'Little Ice Age' summer temperature variations: their nature and relevance to recent global warming trends. *Holocene* 3, 367–376.
- Broecker, W.S., 2000. Was a change in thermohaline circulation responsible for the Little Ice Age? *Proc. Natl. Acad. Sci. Unit. States Am.* 97, 1339–1342.
- Bronk Ramsey, Christopher, 2009. Bayesian analysis of radiocarbon dates. *Radiocarbon* 51, 337–360.
- Bronnimann, S., Franke, J., Nussbaumer, S.U., Zumbuhl, H.J., Steiner, D., Trachsel, M., Heger, G.C., Schurer, A., Worni, M., Malik, A., Fluckiger, J., Raible, C.C., 2019. Last phase of the Little Ice Age forced by volcanic eruptions. *Nat. Geosci.* 12, 650–656.
- Cavitte, M.G.P., Dalaiden, Q., Goosse, H., Lenaerts, J.T.M., Thomas, E.R., 2020. Reconciling the surface temperature–surface mass balance relationship in models and ice cores in Antarctica over the last 2 centuries. *Cryosphere* 14, 4083–4102.
- Cejka, T., Nyvlt, D., Kopalova, K., Bulinova, M., Kavan, J., Lirio, J.M., Coria, S.H., van de Vijver, B., 2020. Timing of the neoglaciation onset on the north-eastern Antarctic peninsula based on lacustrine archive from lake Anonima, Vega island. *Global Planet. Change* 184, 103050.
- Charman, D.J., Amesbury, M.J., Roland, T.P., Royles, J., Hodgson, D.A., Convey, P., Griffiths, H., 2018. Spatially coherent late Holocene Antarctic Peninsula surface air temperature variability. *Geology* 46, 1071–1074.
- Christ, A.J., Talaia-Murray, M., Elking, N., Domack, E.W., Leventer, A., Lavoie, C., Brachfeld, S., Yoo, K.-C., Gilbert, R., Jeong, S.-M., Petrushak, S., Wellner, J., Group, L., 2015. Late Holocene glacial advance and ice shelf growth in Barilari bay, Graham land, West Antarctic peninsula. *Geol. Soc. Am. Bull.* 127, 297–315.
- Clapperton, C.M., Sugden, D.E., 1988. Holocene glacier fluctuations in South America and Antarctica. *Quat. Sci. Rev.* 7, 185–198.
- Consortium, P.K., 2013. Continental-scale temperature variability during the past two millennia. *Nat. Geosci.* 6, 339–345.
- Curl, J.E., 1980. A glacial history of the south Shetland islands, Antarctica. *Institute of Polar Studies Report* 63, 1–129.
- Dalaiden, Q., Goosse, H., Klein, F., Lenaerts, J.T.M., Holloway, M., Sime, L., Thomas, E.R., 2020. How useful is snow accumulation in reconstructing surface air temperature in Antarctica? A study combining ice core records and climate models. *Cryosphere* 14, 1187–1207.
- Davies, B.J., Golleger, N.R., Glasser, N.F., Carrivick, J.L., Ligtenberg, S.R.M., Barrand, N.E., van de Broeke, M.R., Hambrey, M.J., Smellie, J.L., 2014. Modelled glacier response to centennial temperature and precipitation trends on the Antarctic Peninsula. *Nat. Clim. Change* 4, 993–998.
- Davies, B.J., Hambrey, M.J., Glasser, N.F., Holt, T., Rodes, A., Smellie, J.L., Carrivick, J.L., Blockley, S.P.E., 2017. Ice-dammed lateral lake and epishelf lake insights into Holocene dynamics of Marguerite trough ice stream and George VI ice shelf, Alexander island, Antarctic peninsula. *Quat. Sci. Rev.* 177, 189–219.
- Domack, E.W., Ishman, S., Stein, A.B., McClennen, C.E., Jull, A.J.T., 1995. Late Holocene advance of the Muller ice shelf, Antarctic peninsula: sedimentological, geochemical and paleontological evidence. *Antarct. Sci.* 7, 159–170.
- Domack, E., Leventer, A., Dunbar, R., Taylor, F., Brachfeld, S., Sjunneskog, C., ODP Leg 178 Scientific Party, 2001. Chronology of the Palmer Deep site, Antarctic Peninsula: A Holocene palaeoenvironmental reference for the circum-Antarctic. *Holocene* 11, 1–9.
- Etheridge, D.M., Steele, L.P., Langenfelds, R.L., Francey, R.J., Barnola, J.-M., Morgan, V.I., 1996. Natural and anthropogenic changes in atmospheric CO₂ over the last 1000 years from air in Antarctic ice and firn. *J. Geophys. Res.* 101, 4115–4128.
- Fretwell, P.T., Hodgson, D.A., Watcham, E.P., Bentley, M.J., Roberts, S.J., 2010. Holocene isostatic uplift of the south Shetland islands, Antarctic peninsula, modelled from raised beaches. *Quat. Sci. Rev.* 29, 1880–1893.
- Frezzotti, M., Scarchilli, C., Becagli, S., Proposito, M., Urbini, S., 2013. A synthesis of the Antarctic surface mass balance during the last 800 yr. *The Cryosphere* 7, 303–319.
- Gordon, John E., Harkness, Douglas D., 1992. Magnitude and geographic variation of the radiocarbon content in Antarctic marine life: Implications for reservoir corrections in radiocarbon dating. *Quat. Sci. Rev.* 11, 697–708.
- Grove, J.M., 2004. *Little Ice Ages Ancient and Modern*. Routledge, New York.
- Guglielmin, M., Convey, P., Malfasi, F., Cannone, N., 2016. Glacial fluctuations since the 'Medieval warm period' at Rothera point (western Antarctic peninsula). *Holocene* 26, 154–158.
- Hall, B.L., 2007. Late-holocene advance of the Collins ice cap, king George island, South Shetland islands. *Holocene* 17, 1253–1258.
- Hall, B., 2009. Holocene glacial history of Antarctica and the sub-Antarctic islands. *Quat. Sci. Rev.* 28, 2213–2230.
- Hall, B.L., Denton, G.H., 2002. Holocene history of the Wilson Piedmont glacier along the southern coast, Antarctica. *Holocene* 12, 619–627.
- Hall, B.L., Henderson, G.M., Baroni, C., Kellogg, T.B., 2010. Constant Holocene Southern-Ocean ¹⁴C reservoir ages and ice-shelf flow rates. *Earth Planet Sci. Lett.* 296, 115–123.
- Hass, H.C., Kuhn, G., Monien, P., Brumsack, H.-J., Forwick, M., 2010. Climate fluctuations during the past two millennia as recorded in sediments from Maxwell Bay, South Shetland Islands, West Antarctica. In: Howe, J.A., Austin, W.E.N., Forwick, M., Paetzel, M. (Eds.), *Fjord Systems and Archives*. Geological Society, London, pp. 243–260.
- Heaton, T.J., Kohler, P., Butzin, M., Bard, E., Reimer, R.W., Austin, W.E.N., Bronk Ramsey, C., Grootes, P.M., Hughen, K.A., Kromer, B., Reimer, P.J., Adkins, J., Burke, A., Cook, M.S., Olsen, J., Skinner, L.C., 2020. MARINE20 - the marine radiocarbon age calibration curve (0–55,000 cal BP). *Radiocarbon* 62, 779–820.
- Heroy, D.C., Anderson, J.B., 2007. Radiocarbon constraints on Antarctic peninsula ice sheet retreat following the last glacial Maximum (LGM). *Quat. Sci. Rev.* 26, 3286–3297.
- Hodgson, D.A., Roberts, S.J., Smith, J.A., Verleyen, E., Sterken, M., Labarque, M., Sabbe, K., Vyverman, W., Allen, C.S., Leng, M.J., Bryant, C., 2013. Late Quaternary environmental changes in Marguerite Bay, Antarctic Peninsula, inferred from lake sediments and raised beaches. *Quat. Sci. Rev.* 68, 216–236.
- Hogg, A.G., Heaton, T.H., Hua, Q., Palmer, J.G., Turney, C.S.M., Southon, J., Bayliss, A., Blackwell, P.G., Boswijk, G., Bronk Ramsey, C., Pearson, C., Petchey, F., Reimer, P., Reimer, R., Wacker, L., 2020. SHCal20 Southern Hemisphere calibration, 0–55,000 years cal BP. *Radiocarbon* 62, 759–778.
- Ivins, E.R., James, D.P., 2005. Antarctic glacial isostatic adjustment: a new assessment. *Antarct. Sci.* 17, 541–553.
- John, B.S., Sugden, D.E., 1971. Raised marine features and phases of glaciation in the South Shetland Islands. *Br. Antarct. Surv. Bull.* 24, 45–111.
- Johnson, J.S., Bentley, M.J., Roberts, S.J., Binnie, S.A., Freeman, S.P.H.T., 2011. Holocene deglaciation history of the northeast Antarctic Peninsula - a review and new chronological constraints. *Quat. Sci. Rev.* 30, 3791–3802.
- Jones, P.D., Osborn, T.J., Briffa, K.R., 2001. The evolution of climate over the last millennium. *Science* 292, 662–667.
- Jordan, T.A., Riley, T.R., Siddoway, C.S., 2020. The geological history and evolution of West Antarctica. *Nat. Rev.: Earth Environ.* 1, 117–133.
- Kaplan, M.R., Strelin, J.A., Schaefer, J.M., Peltier, C., Martini, M.A., Flores, E., Winckler, G., Schwartz, R., 2020. Holocene glacier behavior around the northern Antarctic Peninsula and possible causes. *Earth Planet Sci. Lett.* 534, 116077.
- Khim, B.-K., Yoon, H.I., Kang, C.Y., Bahk, J.J., 2002. Unstable climate oscillations during the late Holocene in the eastern Bransfield Basin, Antarctic Peninsula. *Quat. Res.* 31, 255–276.
- Kim, S., Yoo, K.-C., Lee, J.I., Khim, B.K., Bak, Y.-S., Lee, M.K., Lee, J., Domack, E.W., Christ, A.J., Yoon, H.I., 2018. Holocene paleogeography of Bigo Bay, west Antarctic Peninsula: Connections between surface water productivity and nutrient utilization and its implication for surface-deep water mass exchange. *Quat. Sci. Rev.* 192, 59–70.
- Kingslake, J., Scherer, R.P., Albrecht, T., Coenen, J., Powell, R.D., Reese, R., Stansell, N.D., Tulaczyk, S., Wearing, M.G., Whitehouse, P.L., 2018. Extensive retreat and re-advance of the west Antarctic ice sheet during the Holocene. *Nature* 558, 430–434.
- Krutz, K.J., Mayewski, P.A., Meeker, L.D., Twickler, M.S., Whitlow, S.I., Pittalwala, I.I., 1997. Biopolar changes in atmospheric circulation during the Little ice age. *Science* 277, 1294–1296.
- Krutz, K.J., Mayewski, P.A., Meeker, L.D., Twickler, M.S., Whitlow, S.I., Pittalwala, I.I., 1997. Bipolar changes in atmospheric circulation during the Little ice age. *Science* 277, 1294–1296.
- Larter, R.D., Barker, P.F., 1991. Effects of ridge crest-trench interaction on Antarctic-Phoenix spreading: forces on a young subducting slab. *J. Geophys. Res.* 96, 19583–19607.
- Leventer, A., Domack, E.W., Ishman, S.E., Brachfeld, S., McClennen, C.E., Manley, P., 1996. Productivity cycles of 200–300 years in the Antarctic Peninsula region: understanding linkages among the sun, atmosphere, oceans, sea ice, and biota. *Geol. Soc. Am. Bull.* 108, 1626–1644.
- Li, Y., Cole-Dai, J., Zhou, L., 2009. Glaciochemical evidence in an East Antarctica ice core of a recent (AD 1450–1850) neoglaciation episode. *J. Geophys. Res.* 114, D08117.
- Lindhorst, S., Schutter, I., 2014. Polar gravel beach-ridge systems: sedimentary architecture, genesis, and implications for climate reconstructions (South Shetland Islands/Western Antarctic Peninsula). *Geomorphology* 221, 187–203.
- Luckman, B.H., 2000. The Little ice age in the Canadian Rockies. *Geomorphology* 32, 357–384.
- Majewski, W., Wellner, J.S., Szczucinski, W., Anderson, J.B., 2012. Holocene oceanographic and glacial changes recorded in Maxwell Bay, West Antarctica. *Mar. Geol.* 326–328, 67–79.
- Mann, M.E., Jones, P.D., 2003. Global surface temperatures over the past two millennia. *Geophys. Res. Lett.* 30, 1820.

- Mann, M.E., Zhang, Z., Rutherford, S., Bradley, R.S., Hughes, M.K., Shindell, D., Ammann, C., Faluvegi, G., Fenbiao, N., 2009. Global signatures and dynamical origins of the Little ice age and Medieval climate anomaly. *Science* 326, 1256–1260.
- Mann, M.E., Steinman, B.A., Brouillette, D.J., Miller, S.K., 2021. Multidecadal climate oscillations during the past millennium driven by volcanic forcing. *Science* 371, 1014–1019.
- Matthews, J.A., Briffa, K.R., 2005. The 'Little ice age': Re-evaluation of an evolving concept. *Geogr. Ann. Phys. Geogr.* 87A, 17–36.
- Michalchuk, B.R., Anderson, J.B., Wellner, J.S., Manley, P., Majewski, W., Bohaty, S., 2009. Holocene climate and glacial history of the northeastern Antarctic Peninsula: the marine sedimentary record from a long SHALDRIL core. *Quat. Sci. Rev.* 28, 3049–3065.
- Miller, G.H., Geirsdottir, A., Zhong, Y., Larsen, D.J., Otto-Biesner, B.L., Holland, M.M., Bailey, D.A., Refsnider, K.A., Lehman, S.J., Southon, J.R., Anderson, C., Bjornsson, H., Thordarson, T., 2012. Abrupt onset of the Little Ice Age triggered by volcanism and sustained by sea-ice/ocean feedbacks. *Geophys. Res. Lett.* 39, L02708.
- Milliken, K.T., Anderson, J.B., Wellner, J.S., Bohaty, S.M., Manley, P.L., 2009. High-resolution Holocene climate record from Maxwell bay, South Shetland islands, Antarctica. *Geol. Soc. Am. Bull.* 121, 1711–1725.
- Minzoni, R.T., Anderson, J.B., Fernandez, R., Wellner, J.S., 2015. Marine record of Holocene climate, ocean, and cryosphere interactions: herbert sound, James Ross island, Antarctica. *Quat. Sci. Rev.* 129, 239–259.
- Morris, E.M., Vaughan, D.G., 2003. Spatial and temporal variation of surface temperature on the Antarctic Peninsula and the limit of viability of ice shelves. *Antarct. Res.* 79, 61–68.
- Mosley-Thompson, E., Thompson, L.G., 1990. Spatial and temporal characteristics of the Little Ice Age: the Antarctic ice core record. In: Weller, G., Wilson, C.L., Severin, B.A.B. (Eds.), *International Conference on the Role of the Polar Regions in Global Change*. University of Alaska, Fairbanks, Alaska (University of Alaska, Fairbanks, Alaska).
- Mulvaney, R., Abram, N.J., Hindmarsh, R.C.A., Arrowsmith, C., Fleet, L., Triest, J., Sime, L.C., Alemay, O., Foord, S., 2012. Recent Antarctic Peninsula Warming Relative to Holocene Climate and Ice-Shelf History. *Nature advance online publication*.
- Murray, A.S., Wintle, A.G., 2000. Luminescence dating of quartz using an improved single-aliquot regenerative-dose protocol. *Radiat. Meas.* 32, 57–73.
- Nesme-Ribes, E., Mangeney, A., 1992. On a plausible physical mechanism linking the Maunder minimum to the Little ice age. *Radiocarbon* 34, 263–270.
- Nield, G.A., Barletta, V.R., Bordon, A., King, M.A., Whitehouse, P.L., Clarke, P.J., Domack, E., Scambos, T.A., Berthier, E., 2014. Rapid bedrock uplift in the Antarctic Peninsula explained by viscoelastic response to recent ice unloading. *Earth Planet. Sci. Lett.* 397, 32–41.
- O Cofaigh, C., Davies, B.J., Livingstone, S.J., Smith, J.A., Johnson, J.S., Hocking, E.P., Hodgson, D.A., Anderson, J.B., Bentley, M.J., Canals, M., Domack, E.W., Dowdeswell, J.A., Evans, J., Glasser, N.F., Hillenbrand, C.D., Larter, R.D., Roberts, S.J., Simms, A.R., 2014. Reconstruction of ice-sheet changes in the Antarctic peninsula since the last glacial Maximum. *Quat. Sci. Rev.* 100, 87–110.
- Ogilvie, A.E.J., Jonsson, T., 2001. 'Little ice age' research: a perspective from Iceland. *Climatic Change* 48, 9–52.
- Oliva, M., Antoniadis, D., Giral, S., Granados, I., Pla-Ribes, S., Toro, M., Liu, E.J., Sanjurjo, J., Vieira, G., 2016. The Holocene deglaciation of the Byers Peninsula (Livingston Island, Antarctica) based on the dating of lake sedimentary records. *Geomorphology* 261, 89–102.
- Orsi, A.J., Cornuelle, B.D., Severinghaus, J.P., 2012. Little ice age cold interval in West Antarctica: evidence from borehole temperature at the west Antarctic ice sheet (WAIS) divide. *Geophys. Res. Lett.* 39, L09710.
- Owens, M.J., Lockwood, M., Hawkins, E., Usoskin, I., Jones, G.S., Barnard, L., Schurer, A., Fasullo, J., 2017. The Maunder Minimum and the Little Ice Age: an update from recent reconstructions and climate simulations. *J. Space Weather Space Clim.* 7, A33.
- Palacios, D., Ruiz-Fernandez, J., Oliva, M., Andres, N., Fernandez-Fernandez, J.M., Schimmelpfennig, I., Leanni, L., Gonzalez-Diaz, B., Team, A., 2020. Timing of formation of neoglacial landforms in the south Shetland islands (Antarctic peninsula): regional and global implications. *Quat. Sci. Rev.* 234, 106248.
- Pike, J., Swann, G.E.A., Leng, M.J., Snelling, A.M., 2013. Glacial discharge along the west Antarctic peninsula during the Holocene. *Nat. Geosci.* 6, 199–202.
- Porter, S.E., Mosley-Thompson, E., Thompson, L.G., Wilson, A.R., 2021. Reconstructing an interdecadal Pacific Oscillation Index from a Pacific basin-wide collection of ice core records. *J. Clim.* 34, 3839–3852.
- Pudsey, C.J., Murray, J.W., Appleby, P., Evans, J., 2006. Ice shelf history from petrographic and foraminiferal evidence, Northeast Antarctic Peninsula. *Quat. Sci. Rev.* 25, 2357–2379.
- Reynolds, J.M., 1981. The distribution of mean annual temperatures in the Antarctic Peninsula. *Br. Antarct. Surv. Bull.* 54, 123–133.
- Rhodes, R.H., Bertler, N.A.N., Baker, J.A., Steen-Larsen, H.C., Sneed, S.B., Morgenstern, U., Johnsen, S.J., 2012. Little Ice Age climate and oceanic conditions of the Ross Sea, Antarctica from a coastal ice core record. *Clim. Past* 8, 1223–1238.
- Roberts, S.J., Hodgson, D.A., Sterken, M., Whitehouse, P.L., Verleyen, E., Vyverman, W., Sabe, K., Balbo, A., Bentley, M.J., Moreton, S.G., 2011. Geological constraints on glacio-isostatic adjustment models of relative sea-level change during deglaciation of Prince Gustav Channel, Antarctic Peninsula. *Quat. Sci. Rev.* 30, 3603–3617.
- Scambos, T., Hulbe, C., Fahnestock, M., 2003. In: *Climate-induced Ice Shelf Disintegration in the Antarctic Peninsula*, Antarctic Peninsula Climate Variability, pp. 79–92.
- Shevenell, A.E., Kennett, J.P., 2002. Antarctic Holocene climate change: A benthic foraminifer stable isotope record from Palmer Deep. *Paleoceanography* 17, 1019.
- Shevenell, A.E., Ingalls, A.E., Domack, E.W., Kelly, C., 2011. Holocene Southern Ocean surface temperature variability west of the Antarctic Peninsula. *Nature* 470, 250–254.
- Simkins, L.M., Simms, A.R., DeWitt, R., 2013. Relative sea-level history of Marguerite Bay, Antarctic Peninsula derived from optically stimulated luminescence-dated beach cobbles. *Quat. Sci. Rev.* 77, 141–155.
- Simms, A.R., DeWitt, R., Kouremenos, P., Drewry, A.M., 2011a. A new approach to reconstructing sea levels in Antarctica using optically stimulated luminescence of cobble surfaces. *Quat. Geochronol.* 6, 50–60.
- Simms, A.R., Alexander, R., Lisiecki, Lorraine, Gebbie, Geoffrey, Whitehouse, Pippa L., Clark, Jordan F., 2019. Balancing the last glacial maximum (LGM) sea-level budget. *Quaternary Science Reviews* 205, 143–153.
- Simms, A.R., Milliken, K.T., Anderson, J.B., Wellner, J.S., 2011b. The marine record of deglaciation of the south Shetland islands, Antarctica since the last glacial Maximum. *Quat. Sci. Rev.* 30, 1583–1601.
- Simms, A.R., Ivins, E.R., DeWitt, R., Kouremenos, P., Simkins, L.M., 2012. Timing of the most recent neoglacial advance and retreat in the south Shetland islands, Antarctic peninsula: insights from raised beaches and Holocene uplift rates. *Quat. Sci. Rev.* 47, 41–55.
- Simms, A.R., Whitehouse, P.L., Simkins, L.M., Nield, G.A., DeWitt, R., Bentley, M.J., 2018. Late Holocene relative sea levels near Palmer Station, northern Antarctic Peninsula, strongly controlled by late Holocene ice-mass changes. *Quat. Sci. Rev.* 199, 49–59.
- Smith, R.I.L., 1982. Plant succession and re-exposed moss banks on a deglaciated headland in Arthur Harbour, Anvers Island. *Br. Antarct. Surv. Bull.* 51, 193–199.
- Stenni, B., Curran, M.A.J., Abram, N.J., Orsi, A., Goursaud, S., Masson-Delmotte, V., Neukom, R., Goosse, H., Divine, D., van Ommen, T., Steig, E.J., Dixon, D.A., Thomas, E.R., Bertler, N.A.N., Isaksson, E., McKay, A., Werner, M., Frezzotti, M., 2017. Antarctic climate variability on regional and continental scales over the last 2000 years. *Clim. Past* 13, 1609–1634.
- Sterken, M., Roberts, S.J., Hodgson, D.A., Vyverman, W., Balbo, A.L., Sabe, K., Moreton, S.G., Verleyen, E., 2012. Holocene glacial and climate history of prince Gustav channel, northeastern Antarctic peninsula. *Quat. Sci. Rev.* 31, 93–111.
- Stuiver, M., Reimer, P.J., Reimer, R.W., 2021. CALIB 8.2 (WWWW program).
- Sugden, D.E., John, B., 1973. In: *The Ages of Glacier Fluctuations in the South Shetland Islands, Antarctica, Palaeoecology of Africa, the Surrounding Islands and Antarctica*. Balkema, Cape Town, pp. 141–159.
- Tavernier, I., Verleyen, E., Hodgson, D.A., Heirman, K., Roberts, S.J., Imura, S., Kudoh, S., Sabe, K., de Batist, M., Vyverman, W., 2014. Absence of a Medieval climate anomaly, Little ice age and twentieth century warming in skarvnsnes, Lutzow holm bay, east Antarctica. *Antarct. Sci.* 26, 585–598.
- The RAISED Consortium, Bentley, M.J., O Cofaigh, C., Anderson, J.B., Conway, H., Davies, B., Graham, A.G.C., Hillenbrand, C.D., Hodgson, D.A., Jamieson, S.R., Larter, R.D., Mackintosh, A., Smith, J.A., Verleyen, E., Ackert, R.P., Bart, P.J., Berg, S., Brunstein, D., Canals, M., Colhoun, E.A., Crosta, X., Dickens, W.A., Domack, E.W., Dowdeswell, J.A., Dunbar, R., Ehrmann, W., Evans, J., Favier, V., Fink, D., Fogwill, C.J., Glasser, N.F., Gohl, K., Gollledge, N.R., Goodwin, I., Gore, D.B., Greenwood, S.L., Hall, B.L., Hall, K., Hedding, D.W., Hein, A.S., Hocking, E.P., Jakobsson, M., Johnson, J.S., Jomelli, V., Jones, R.S., Klages, J.P., Kirstoffersen, Y., Kuhn, G., Leventer, A., Licht, K., Lilly, K., Lindow, J., Livingstone, S.J., Masse, G., McGlone, M.S., McKay, R.M., Melles, M., Miura, H., Mulvaney, R., Nel, W., Nitsche, F.O., O'Brien, P.E., Post, A.L., Roberts, S.J., Saunders, K.M., Selkirk, P.M., Simms, A.R., Spiegel, C., Stollendorf, T.D., Sugden, D.E., van der Putten, N., van Ommen, T., Verfaillie, D., Vyverman, W., Wagner, B., White, D.A., Witus, A.E., Zwart, D., 2014. A community-based geological reconstruction of Antarctic ice sheet deglaciation since the last glacial Maximum. *Quat. Sci. Rev.* 100, 1–9.
- Thomas, E.R., Marshall, G.J., McConnell, J.R., 2008. A doubling in snow accumulation in the western Antarctic peninsula since 1850. *Geophys. Res. Lett.* 35, L01706. <https://doi.org/10.1029/2007GL032529>.
- Thomas, E.R., Hosking, J.S., Tuckwell, R.R., Warren, R.A., Ludlow, E.C., 2015. Twentieth century increase in snowfall in coastal West Antarctica. *Geophys. Res. Lett.* 42, 9387–9393. <https://doi.org/10.1002/2015GL065750>.
- Thomas, Elizabeth R., Tetzner, Dieter R., 2018. The climate of the Antarctic Peninsula during the twentieth century: Evidence from ice cores. In: Kanao, Masaki, Toyokuni, Genti, Yamamoto, Masa-yuki (Eds.), *Antarctica - A Key to Global Change*. Intech.
- Thomas, E.R., Van Wessel, J.M., Roberts, J., Isaksson, E., Schlosser, E., Fudge, T.J., Vallelonga, P., Medley, B., Lenaerts, J., Bertler, N., Van den Broeke, M.R., Dixon, D.A., Frezzotti, M., Stenni, B., Curran, M., McKay, A.A., 2017. Regional Antarctic snow accumulation over the past 1000 years. *Clim. Past* 13, 1491–1513.
- Thompson, L.G., Peel, D.A., Mosley-Thompson, E., Dai, J., Lin, P.N., Davis, M.E., Raymond, C.F., 1994. Climate since AD 1510 on dyer plateau, Antarctic peninsula: evidence for recent climate change. *Ann. Glaciol.* 20, 420–426.
- Turner, J., Phillips, T., Thamban, M., Rahaman, W., Marshall, G.J., Wille, J.D., Favier, V., Winton, H.L., Thomas, E., Wang, Z., van den Broeke, M., Hosking, S., Lachlan-Cope, T., 2019. The dominant role of extreme precipitation events in Antarctic snowfall variability. *Geophys. Res. Lett.* 46, 3502–3511.
- van Wessel, J.M., Ligtenberg, S.R.M., Reijmer, C.H., Van de Berg, W.J., Van den

- Broeke, M.R., Barrand, N.E., Thomas, E.R., Turner, J., Wuite, J., Scambos, T.A., Van Meijgaard, E., 2016. The modelled surface mass balance of the Antarctic Peninsula at 5.5 km horizontal resolution. *Cryosphere* 10, 271–285.
- Vaughan, D.G., Marshall, G.J., Connolley, W.M., Parkinson, C., Mulvaney, R., Hodgson, D.A., King, J.C., Pudsey, C.J., Turner, J., 2003. Recent rapid regional climate warming on the Antarctic Peninsula. *Climate Change* 60, 243–274.
- Wanner, H., Solomina, O., Grosjean, M., Ritz, S.P., Jetel, M., 2011. Structure and origin of Holocene cold events. *Quat. Sci. Rev.* 30, 3109–3123.
- Wintle, A.G., Murray, A.S., 2006. A review of quartz optically stimulated luminescence characteristics and their relevance in single-aliquot regeneration dating protocols. *Radiat. Meas.* 41, 369–391.
- Wolfl, A.-C., Wittenberg, N., Feldens, P., Hass, H.C., Betzler, C., Kuhn, G., 2016. Submarine landforms related to glacier retreat in a shallow Antarctic fjord. *Antarct. Sci.* 28, 475–486.
- Yoo, K.-C., Yoon, H.I., Kim, J.-K., Khim, B.-K., 2009. Sedimentological, geochemical and palaeontological evidence for a neoglacial cold event during the late Holocene in the continental shelf of the northern South Shetland Islands, West Antarctica. *Polar Res.* 28, 177–192.
- Yoon, H.I., Yoo, K.-C., Bak, Y.-S., Lim, H.S., Kim, Y., Lee, J.I., 2010. Late Holocene cyclic glaciomarine sedimentation in a subpolar fjord of the South Shetland Islands, Antarctica, and its paleoceanographic significance: Sedimentological, geochemical, and paleontological evidence. *Geol. Soc. Am. Bull.* 122, 1298–1307.
- Yu, Z., Beilman, D.W., Loisel, J., 2016. Transformations of landscape and peat-forming ecosystems in response to late Holocene climate change in the western Antarctic Peninsula. *Geophys. Res. Lett.* 43, 7186–7195.
- Zhang, M., Ren, J., Cheng, G., Li, Z., Xia, C., Qin, D., Kang, J., Li, J., 2002. Temperature variation and its driving forces over the Antarctic coastal regions in the past 250 years. *J. Geogr. Sci.* 12, 379–386.
- Zhong, Y., Miller, G.H., Otto-Biesner, B.L., Holland, M.M., Bailey, D.A., Schneider, D.P., Geirsdottir, A., 2011. Centennial-scale climate change from decadal-paced explosive volcanism: a coupled sea ice-ocean mechanism. *Clim. Dynam.* 37, 2373–2387.
- Zurbuchen, J., Simms, A.R., 2019. Late Holocene ice-mass changes recorded in a relative sea-level record from Joinville Island, Antarctica. *Geology* 47, 1064–1068.